# Nanocellulose: Rheology and Applications

Alain Dufresne

Univ. Grenoble Alpes, CNRS, Grenoble INP, LGP2, F-38000, France

Nordic Rheology Conference,
Gothenburg, August 21-23, 2019

# Outlines

- Cellulose nanomaterials
- Dynamic rheological behavior
- Rheology of aqueous suspensions
- Birefringence/chiral nematic behavior
- Solid state rheology of cellulose/polymer nanocomposites
    - ☑ What can we learn from the storage modulus?
    - ☑ What can we learn from the loss angle?

# Cellulose Nanomaterials

Mechanically-induced deconstructing strategy

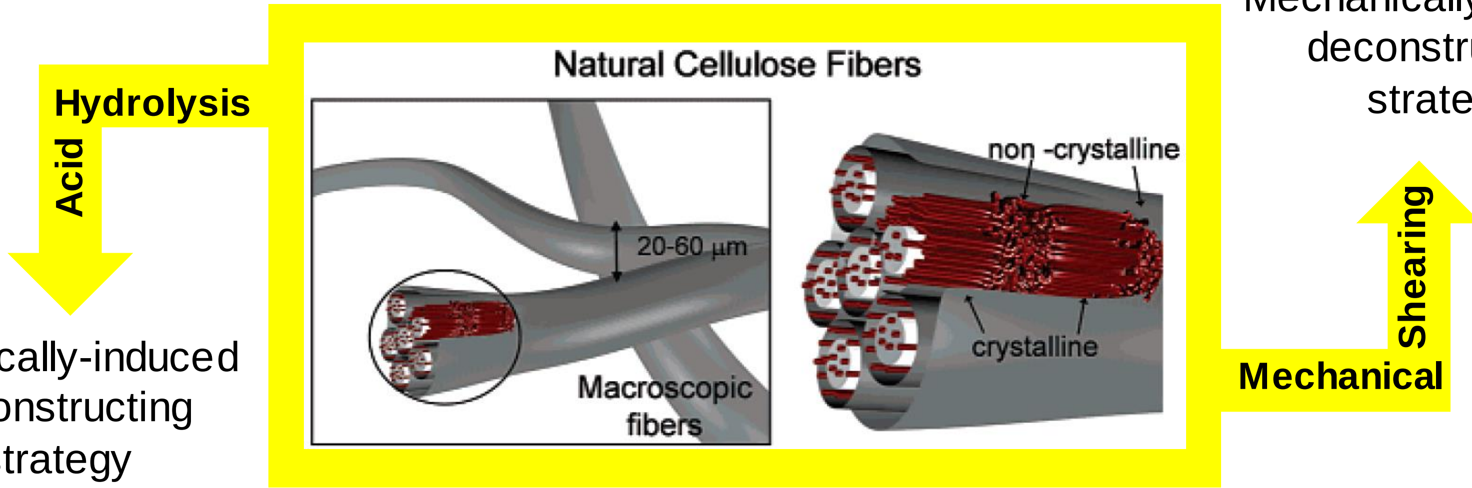


Chemically-induced deconstructing strategy

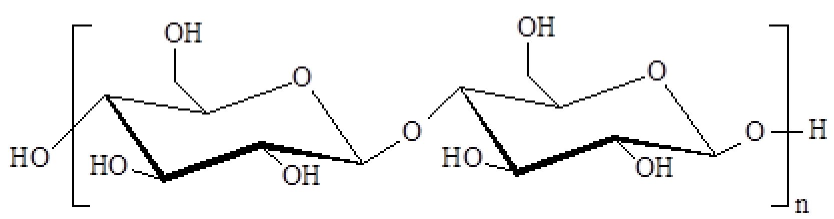

# Mechanically-induced deconstructing strategy

## Homogenizer

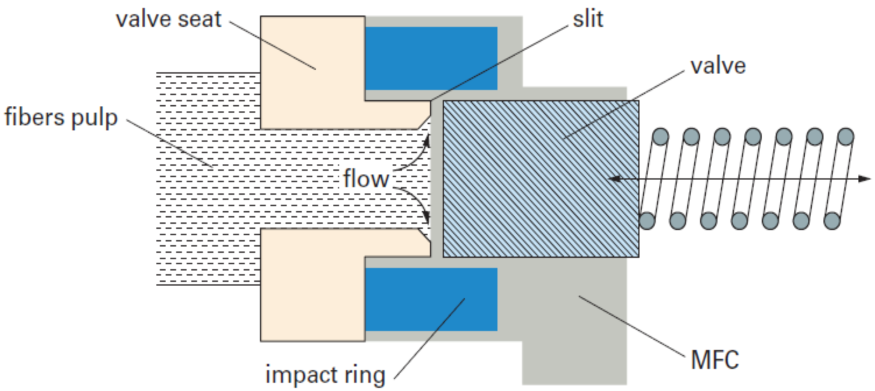


## Aqueous counter collision

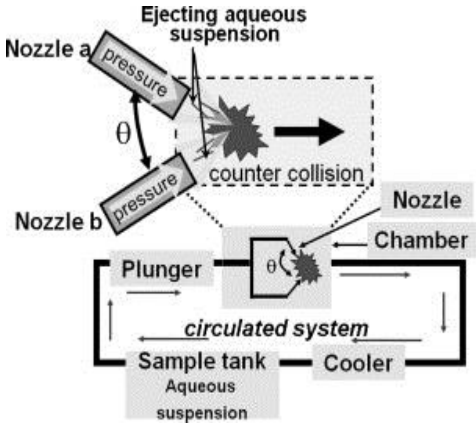


## Microfluidizer (Microfluidics Inc., USA)

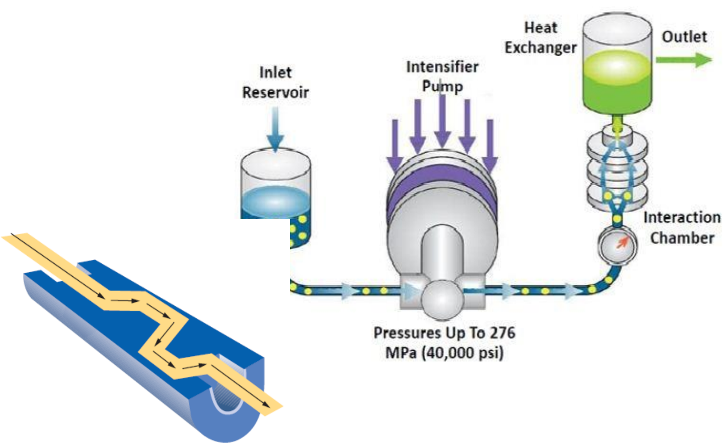


## Ultra-fine friction grinder Masuko Supermasscolloider

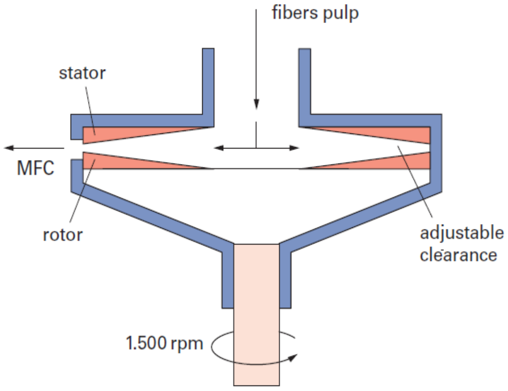

# Cellulose Nanofibrils

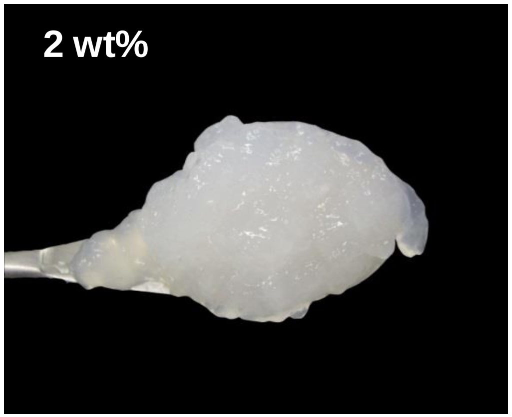


Lavoine et al., *Carbohydr. Polym*. **2012**, 90, 735-764


Malainine et al., *Compos. Sci. Technol.* **2005**, 65, 1520-1526

Stability in water due to residual hemicelluloses

Viscous gel with shear-thinning behavior

**High energy demand**

30,000 kWh/ton (Nakagaito and Yano, 2004)

70,000 kWh/ton (Eriksen et al, 2008)

→ **necessity of a pretreatment**

enzymatic hydrolysis

Carboxymethylation

TEMPO-catalyzed oxidation pretreatment

Cryocrushing

**Width ~ 2-100 nm**
**Length ?**

# Chemically-induced Deconstructing Strategy

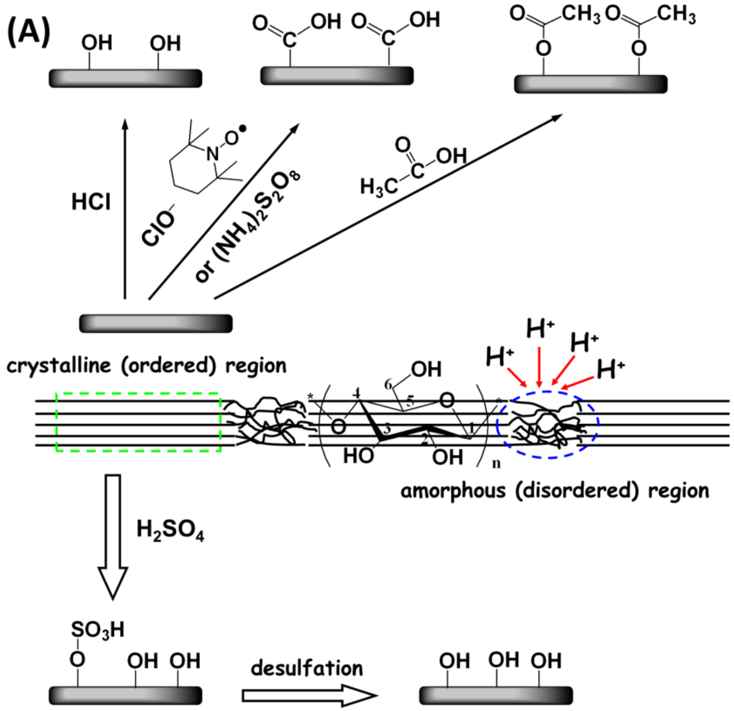


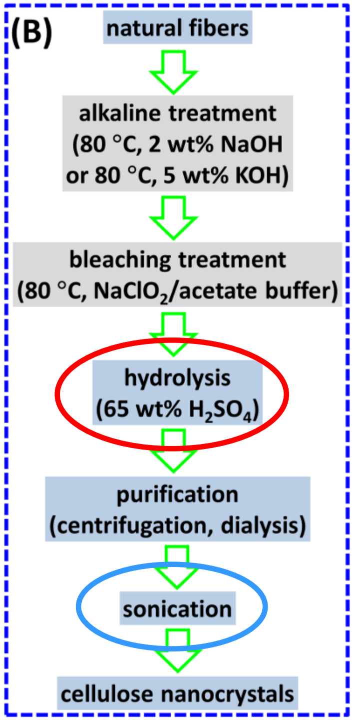


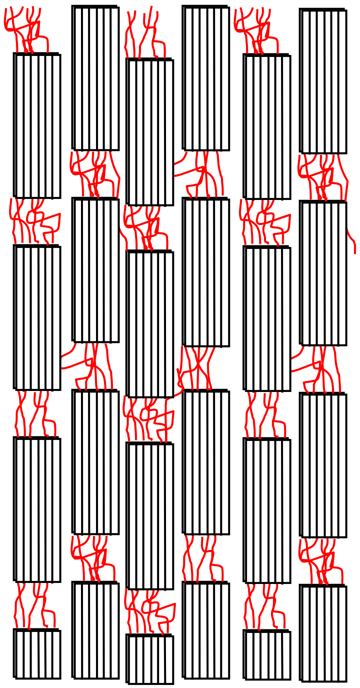

Stability in water due to surface sulfate groups

**Width ~ few nm**
**Length ~ few 100 nm**

# Cellulose Nanocrystals

*Ramie fibers*

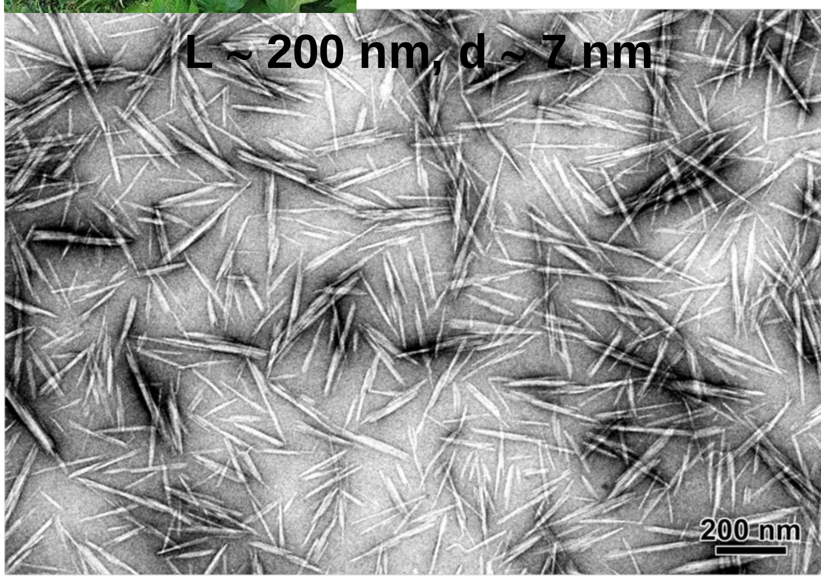


Habibi et al., *J. Mater. Chem.* **2008**, 18, 5002-5010

*Tunicate*

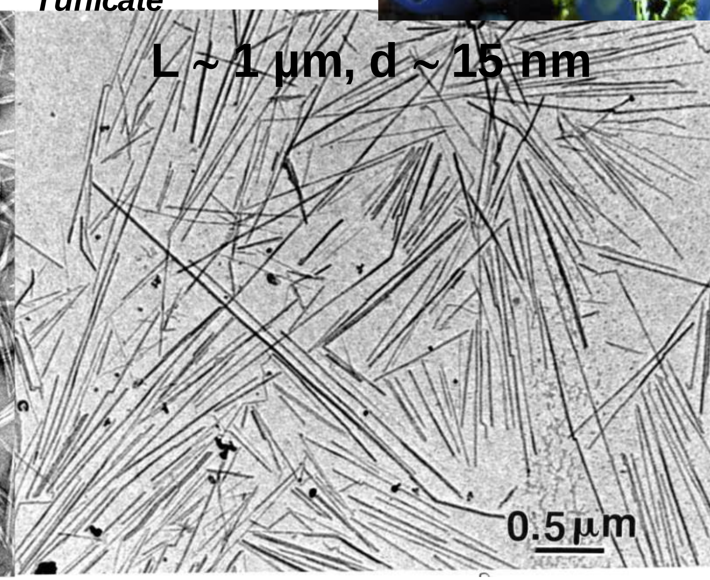


Anglès and Dufresne, *Macromolecules* **2000**, 33, 8344-8353

# Applications of Cellulose Nanomaterials

Coatings

Adhesives

Energy

Inks/printing

Pulp & paper

Composites

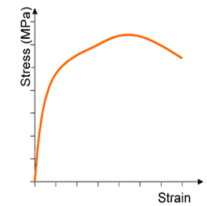


Films

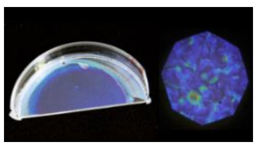

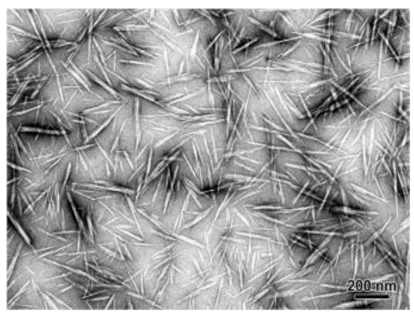



Electronics

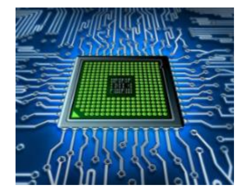

Biomedical

Filtration

Emulsions

Cosmetics

Food industry

Packaging

Construction

Textiles

# Dynamic Rheological Behavior

Can be applied over a broad range of viscosity (solid/liquid)

Useful for observing the viscoelastic nature of the material

An oscillating force is applied to a sample of material and the resulting displacement of the sample is measured

The stiffness of the sample can be determined, and the sample modulus can be calculated

By measuring the time lag in the displacement compared to the applied force it is possible to determine the damping properties of the material

# Dynamic Rheological Behavior

By applying a stress that varies sinusoidally with time, a viscoelastic material will respond with a sinusoidal strain for low stress amplitude

This strain is out of phase with the applied stress, by the phase angle $\delta$ (phase lag due to the excess time necessary for molecular motions and relaxations to occur)

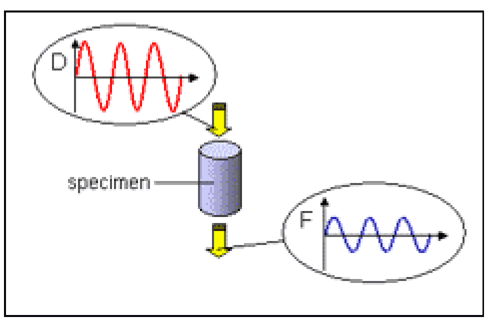


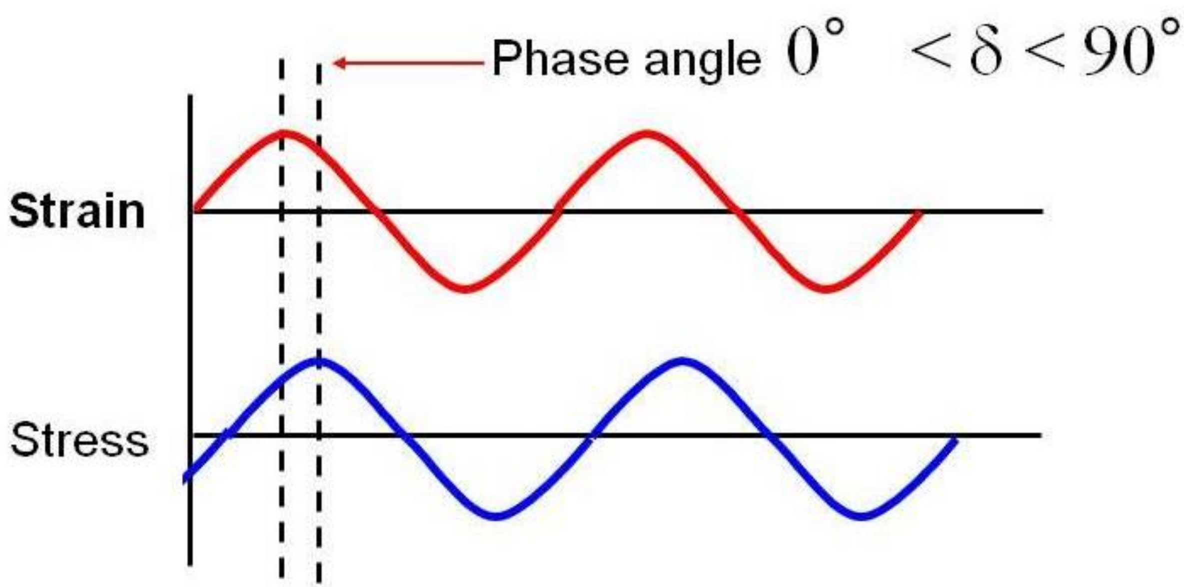

# Dynamic Rheological Behavior

$$\sigma = \sigma_o \sin(\omega t + \delta) \qquad \sigma = \sigma_o \sin(\omega t)$$

$$\varepsilon = \varepsilon_o \sin(\omega t) \qquad \varepsilon = \varepsilon_o \sin(\omega t - \delta)$$

$\omega$ = angular frequency

$$\sigma = \sigma_o \cos\delta \sin(\omega t) + \sigma_o \sin\delta \cos(\omega t)$$

in-phase component ($\sigma_o \cos\delta$) — out-of-phase component ($\sigma_o \sin\delta$)

$$\sigma = \varepsilon_o E' \sin(\omega t) + \varepsilon_o E'' \cos(\omega t)$$

$$E' = \frac{\sigma_o}{\varepsilon_o}\cos\delta = \text{in-phase modulus}$$

$$E'' = \frac{\sigma_o}{\varepsilon_o}\sin\delta = \text{out-of-phase modulus}$$

LGP2

# Dynamic Rheological Behavior

$$\sigma^* = \sigma_o \exp i(\omega t + \delta)$$

$$\varepsilon^* = \varepsilon_o \exp(i\omega t)$$

$$E^* = \frac{\sigma^*}{\varepsilon^*} = \frac{\sigma_o}{\varepsilon_o} e^{i\delta} = \frac{\sigma_o}{\varepsilon_o}(\cos\delta + i\delta) = E' + iE''$$

E' = storage modulus (describes ability of material to store potential energy and release it upon deformation) → stiffness ~ Young's modulus

E'' = loss modulus (associated with energy dissipation in the form of heat upon deformation) → internal friction ~ molecular motions, relaxation processes

tan δ = E''/E' = tangent of the phase angle

**DYNAMIC PROPERTIES PROVIDE INFORMATION AT THE MOLECULAR LEVEL TO UNDERSTAND THE MACROSCOPIC MECHANICAL BEHAVIOR**

# Applications of Cellulose Nanomaterials

Important features of cellulose nanomaterials for use as rheology-modifier

High specific area

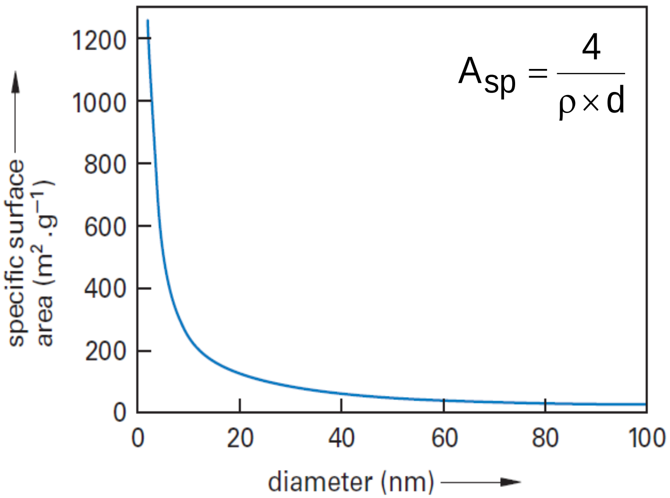


Dufresne, *Nanocellulose* **2017**, 2nd Ed., Berlin/ Boston: Walter de Gruyter GmbH & Co KG

High density of surface OH groups

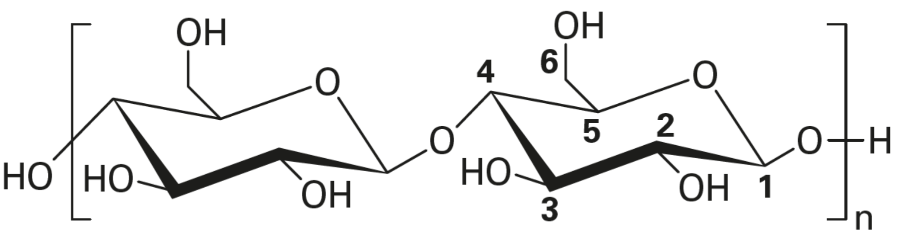


Strong interaction with polar liquid when in suspension

# Impact of Concentration


Lavoine et al., *Carbohydr. Polym*. **2012**, *90*, 735-764

**Applications**
Food, cosmetic, pharmaceutical industries

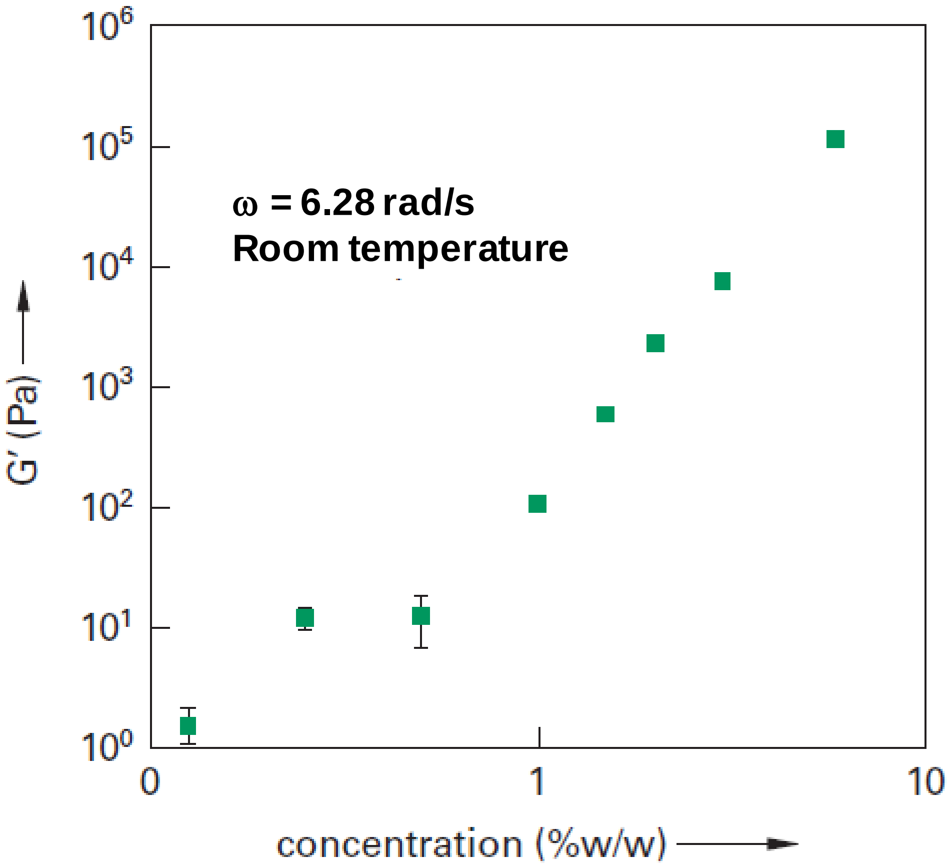


Pääkkö et al., *Biomacromolecules* **2007**, 8, 1934-1941

# Impact of Concentration

G' (solid symbols) / G" (open symbols)

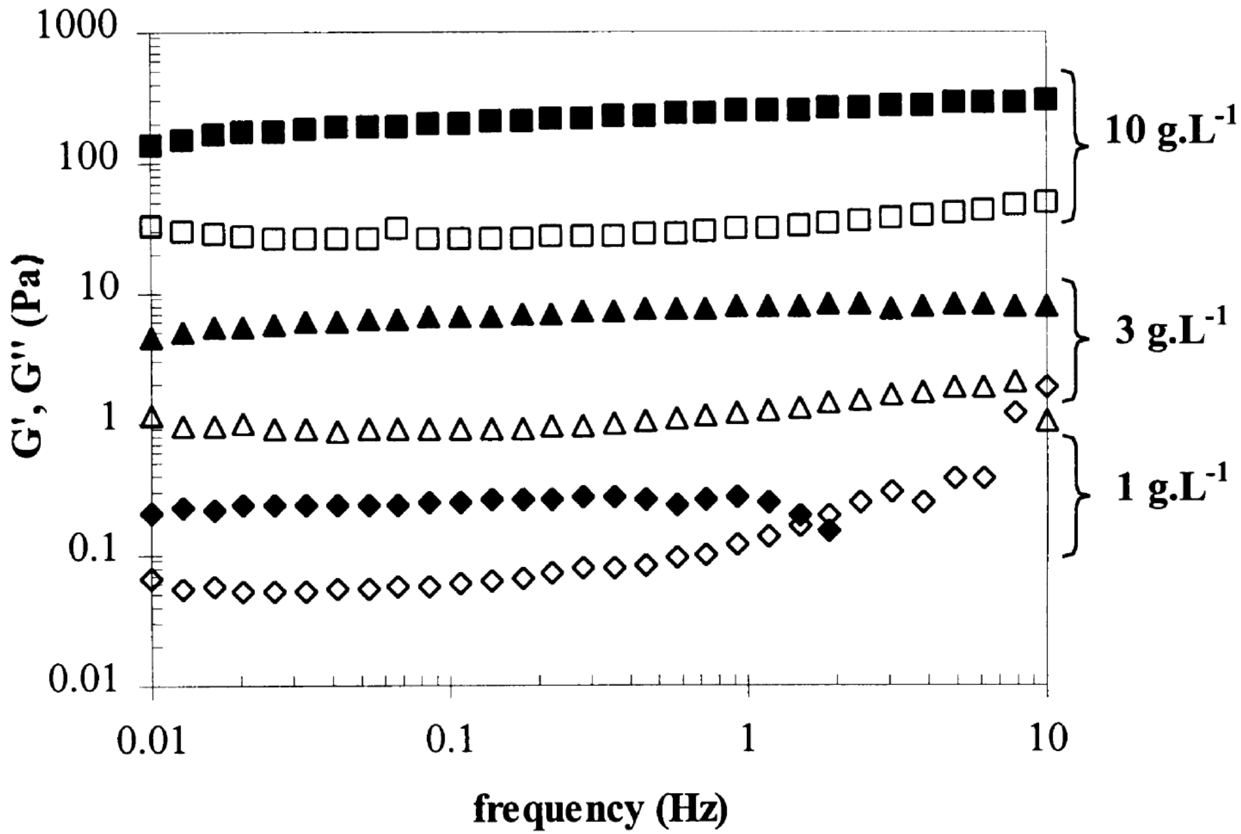


G' > G" a physical network is formed due to mechanical entanglements between nanofibrils

Lowys et al., *Food Hydrocoll.* **2001**, 15, 25-32

# Impact of Temperature

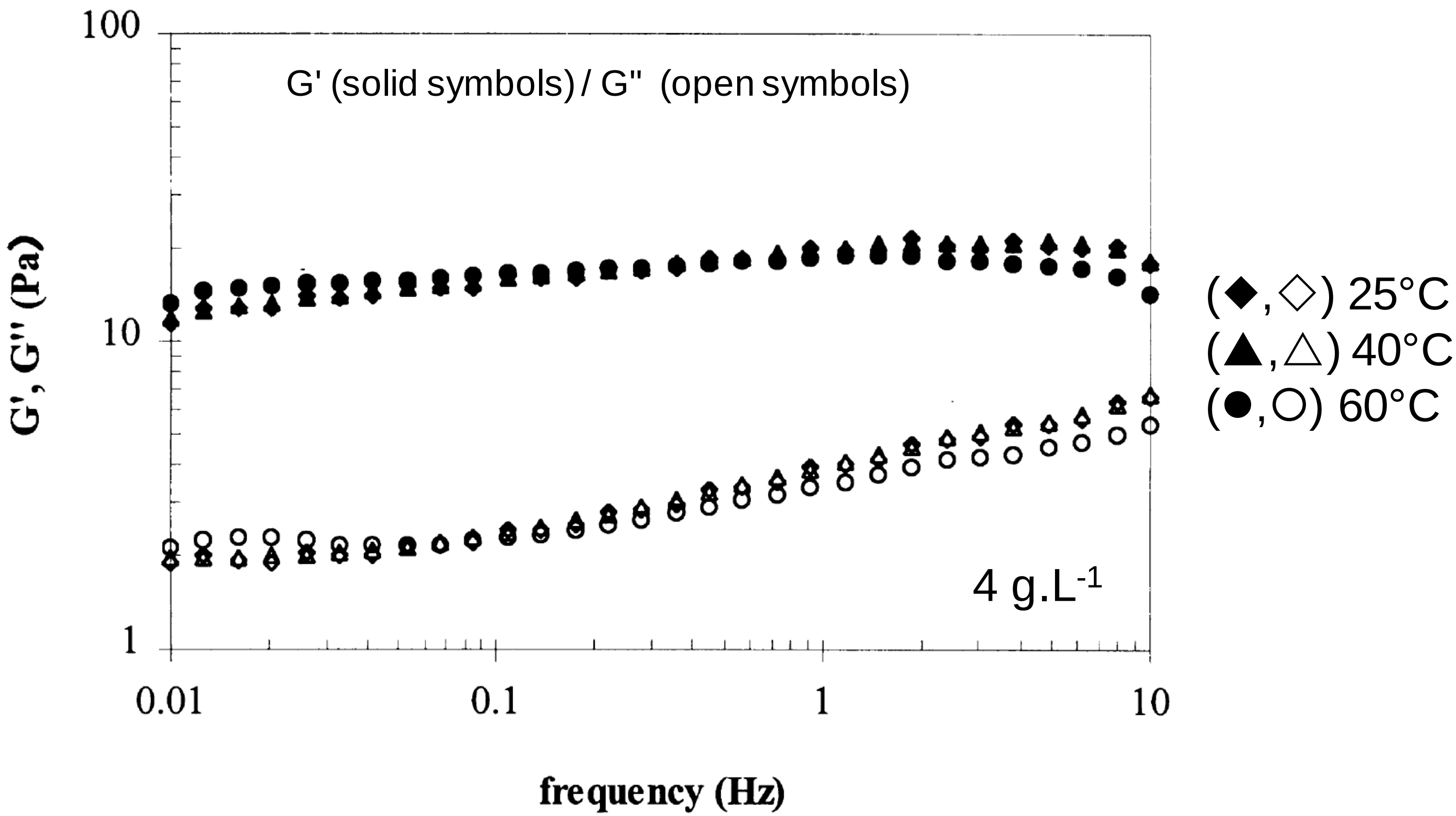


Lowys et al., *Food Hydrocoll.* **2001**, 15, 25-32

# Impact of Oxidation

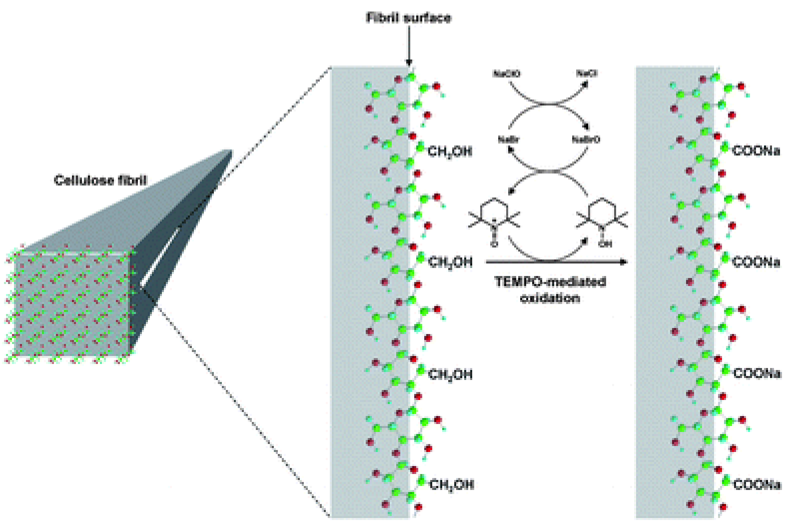


Schematic model for the oxidation of C6 primary hydroxyls on native cellulose nanofibrils surface to C6 carboxylate groups using the TEMPO/NaBr/NaClO system

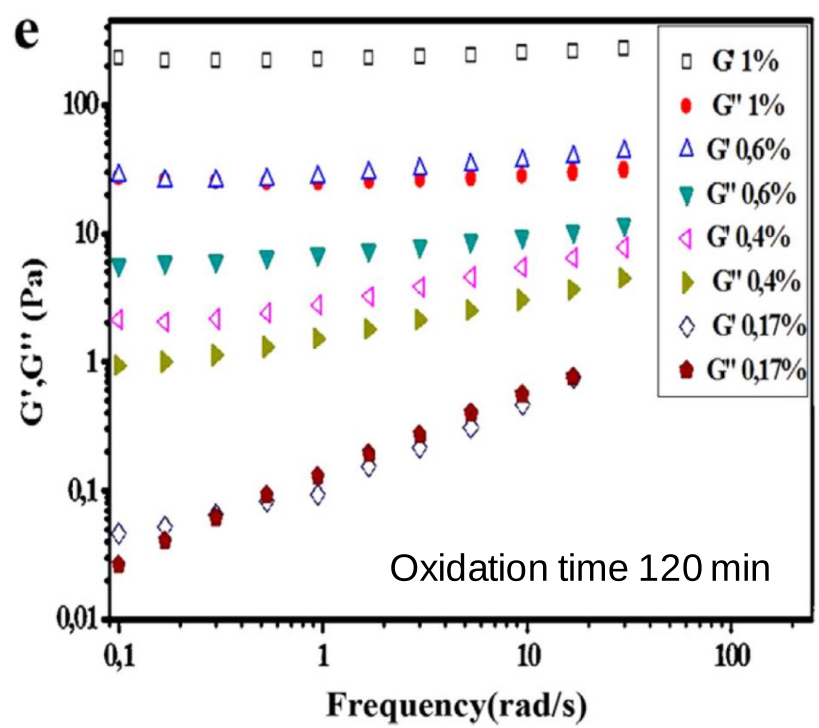


1 Hz

Okita et al., *Biomacromolecules* **2010**, 11, 1696-1700

Benhamou et al., *Carbohydr. Polym.* **2014**, 99, 74-83

# Impact of Oxidation

| Reaction Time (min) | COONa Content (µmol.g$^{-1}$) | DP |
|---|---|---|
| 0 | 177 | 650 |
| 5 | 221 | 500 |
| 15 | 265 | 390 |
| 30 | 442 | 215 |
| 60 | 575 | 130 |
| 120 | 774 | 100 |

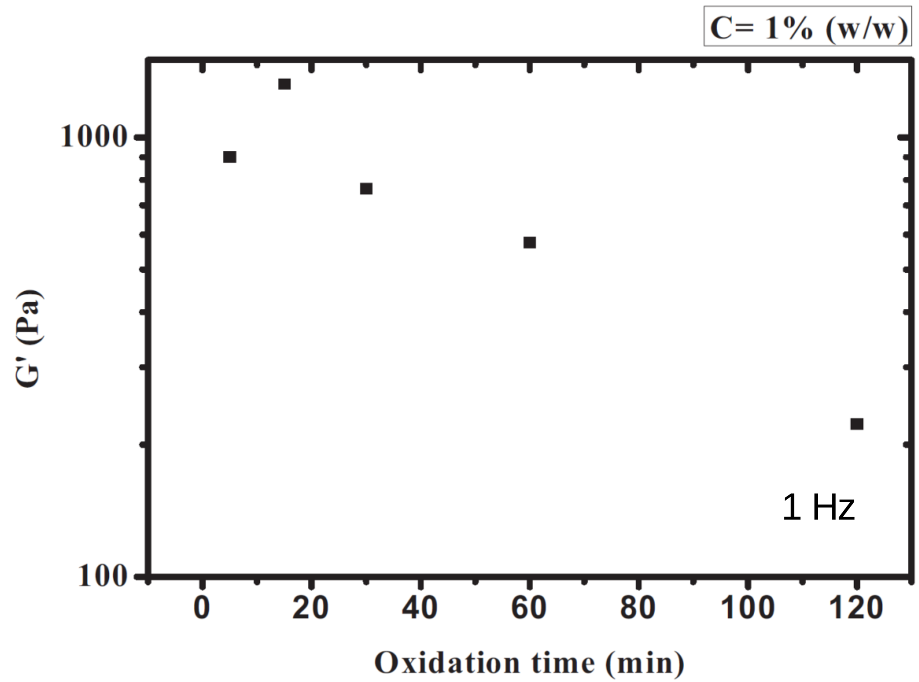


Increase in CNF surface charge → stronger immobilization of surrounding water molecules
→ higher gel stiffness

Decrease of CNF length → lower gel stiffness

Benhamou et al., *Carbohydr. Polym.* **2014**, 99, 74-83

# Birefringence – Chiral Nematic Behavior

A CNC suspension in water at low concentrations forms a clear stable isotropic fluid

At higher concentrations the CNCs self-align to form a chiral nematic liquid crystalline phase in equilibrium with isotropic phase


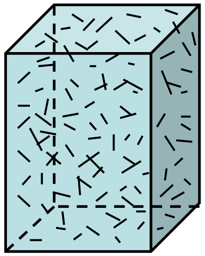

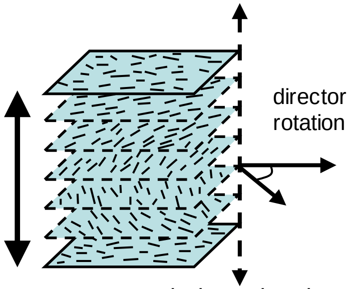


Marchessault et al., *Nature* **1959**, *184*, 632-633

Revol et al., *Int. J. Biol. Macromol*. **1992**, 14, 170-172

Siqueira et al., *Cellulose* **2010**, 17, 289-298

# Birefringence – Chiral Nematic Behavior

$\lambda = n P \sin \theta$

(P controlled through ionic strength, T, concentration, exposure to magnetic field and US treatment)

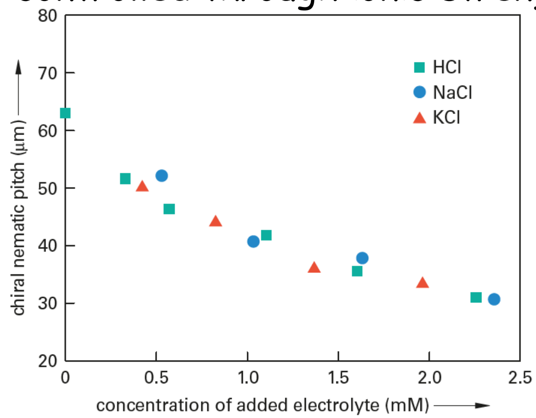


Dong et al., *Langmuir* **1996**, 12, 2076-2082

Slow evaporation produces semi-translucent films that retain the self-assembled chiral nematic liquid crystalline order formed in the suspension

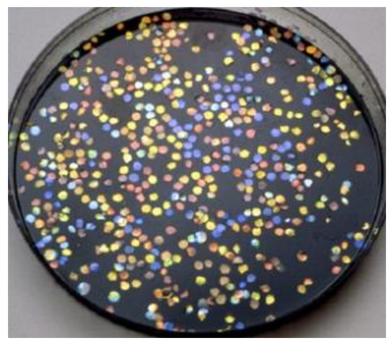

Mixture of confettis cut from CNC films prepared with different NaCl concentrations, thus giving different reflection wavelengths

Revol et al., *US Patent 5,629,055*, **1997**

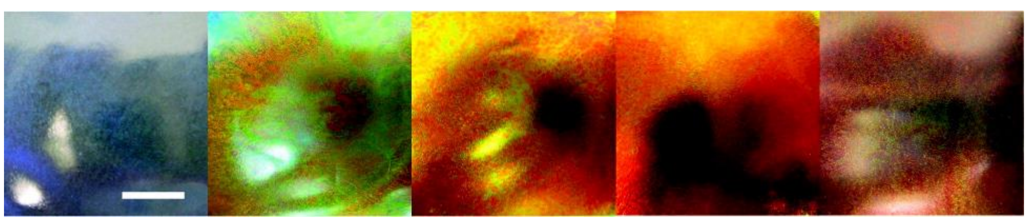

CNC films produced from suspensions treated with increasing applied ultrasonic energy (0, 250, 700, 1800, and 7200 J/g CNC) from left to right
Scale marker = 1 cm

Beck et al., *Biomacromolecules* **2011**, 12, 167-172

## Applications

Security papers

UV or IR reflective barriers

# Applications of Cellulose Nanomaterials

Important features of cellulose nanomaterials for use as reinforcement for polymeric matrices

High specific surface area (~ 100 $m^2.g^{-1}$)
High aspect ratio
High modulus/strength (E = 130/100 GPa for CNC/CNF)
Lightweight (density = 1.5 $g.cm^{-3}$)
Surface functionalization

# Solid State Rheology

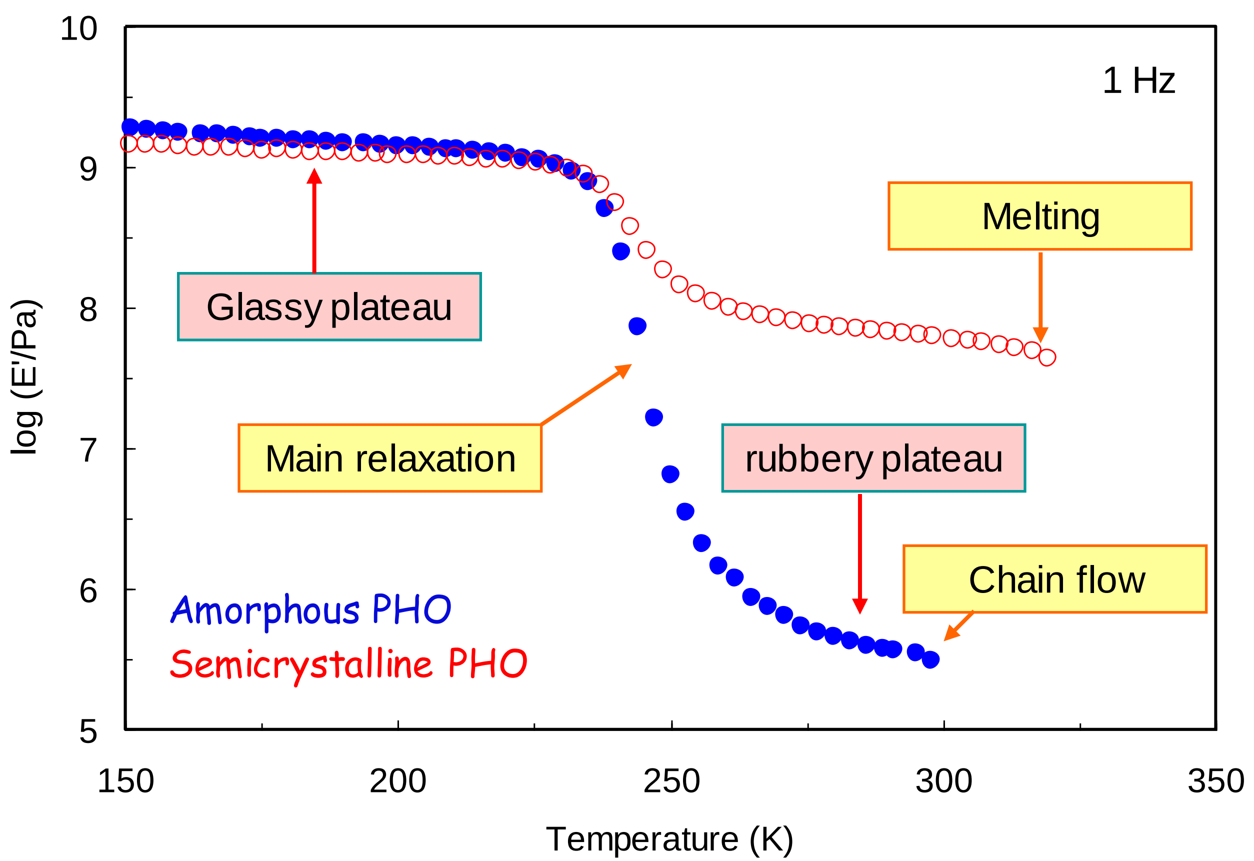


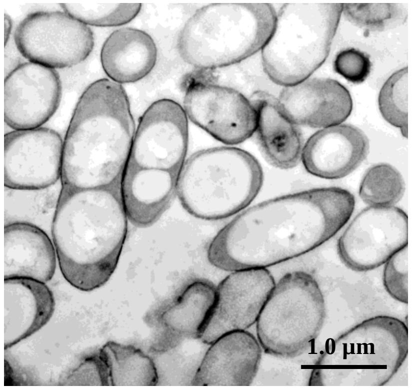


**Semicrystalline polymer**

(i) rubbery modulus known to depend on $\chi c$ (filler)

(ii) flow = melting

(physical crosslinks)

# Solid State Rheology

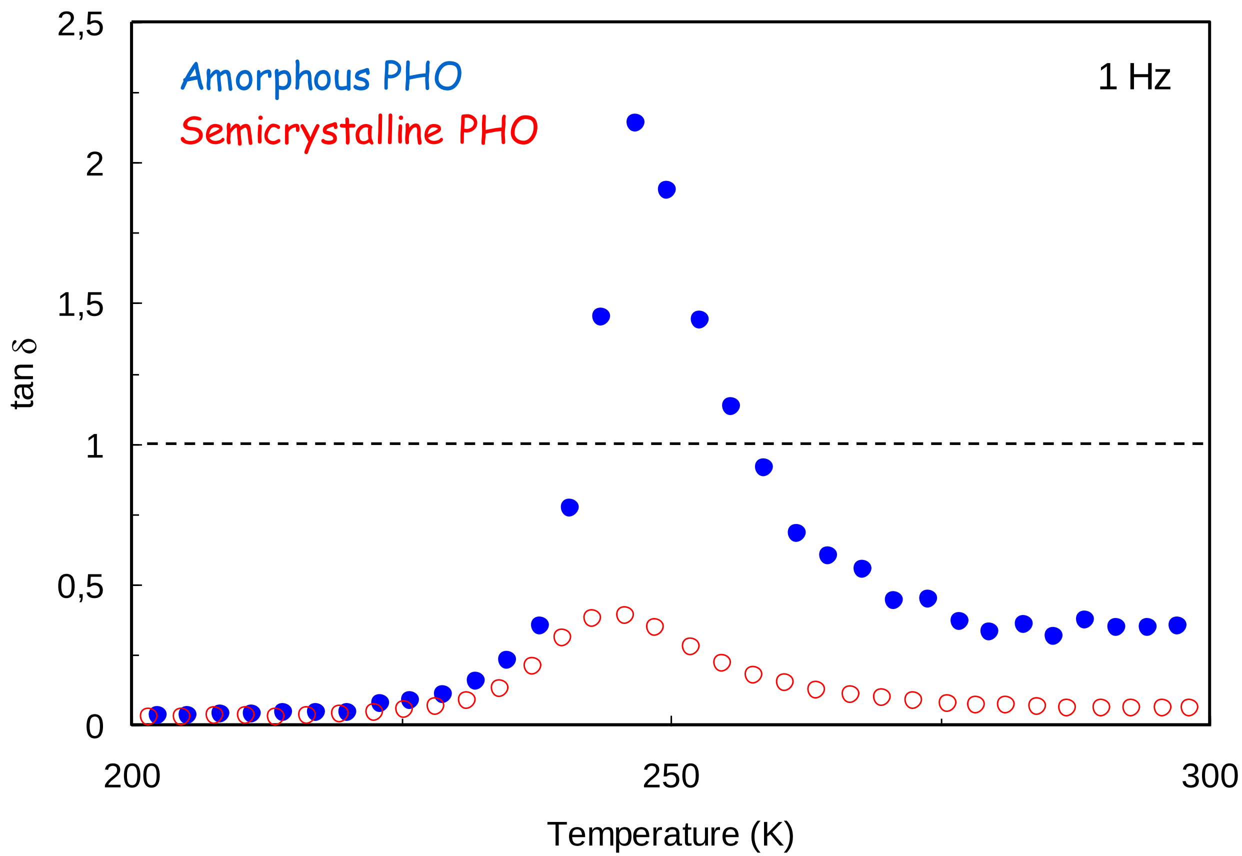


**Max tan δ ($T_\alpha$)**

(i) number of mobile units

(ii) magnitude of modulus drop

# Transition vs. Relaxation

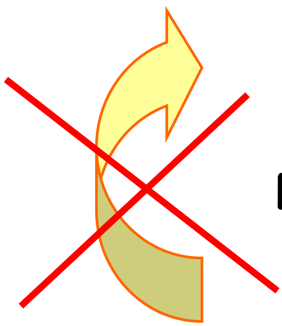

**Transition** = change from one physical state to another

1st order : melting, crystallization

~ 2nd order : glass-rubber transition

**Relaxation** = reversible and detectable phenomenon resulting from a change of molecular mobility

Main relaxation associated to Tg

Secondary relaxations (lateral groups, crankshaft)

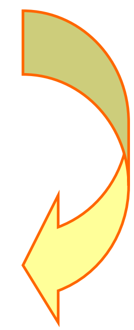

# Properties of Multiphase Materials

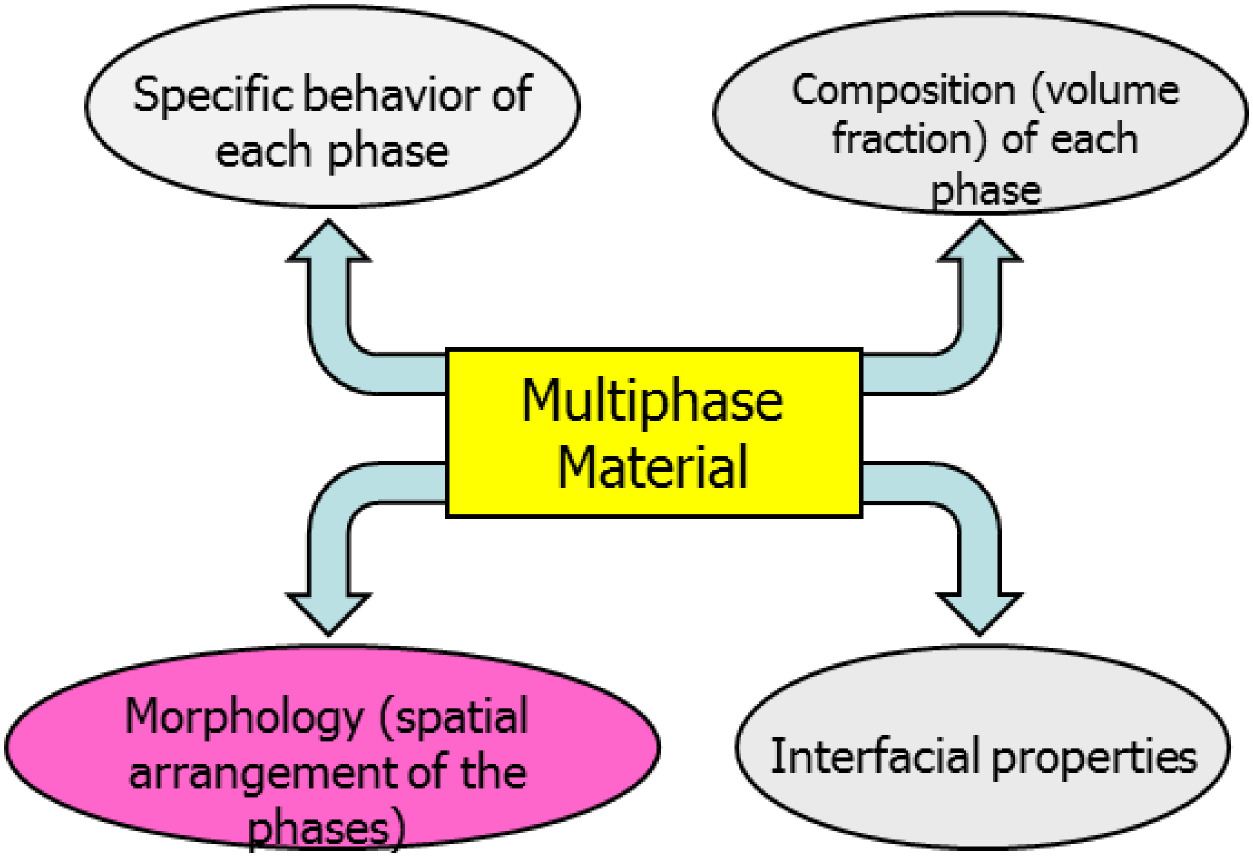

# Flow-chart for the Study of Multiphase Materials

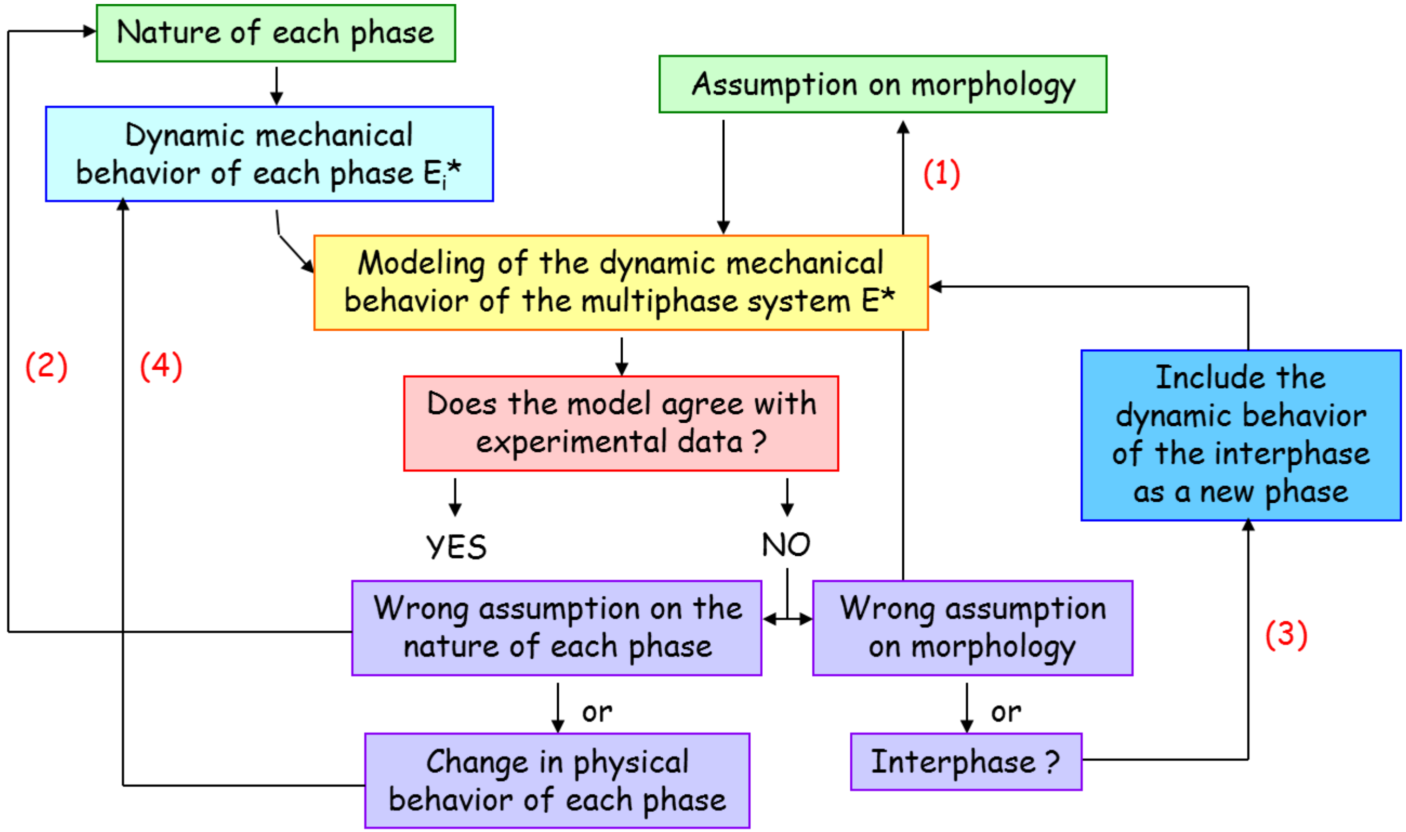


(1) Morphology (2) Chemical composition of each phase (3) Interphase between main phases
(4) Possible change in physical properties of each phase

# Rheology of Cellulose/Polymer Nanocomposites

Tunicin CNC/poly(S-co-BuA) latex

water evaporation (T>Tg) → particle coalescence
→ nanocomposite film

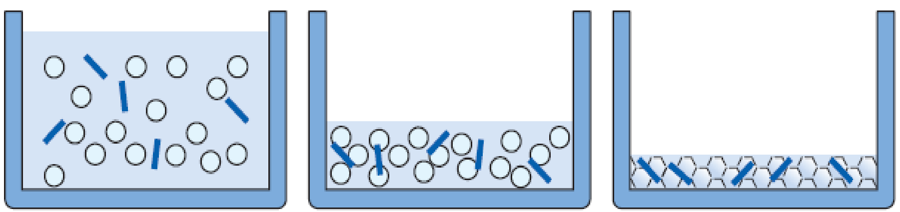

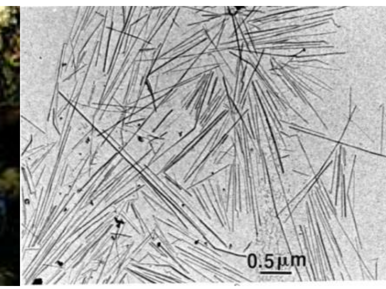


L ~ 1 µm, d ~ 15 nm
L/d ~ 67

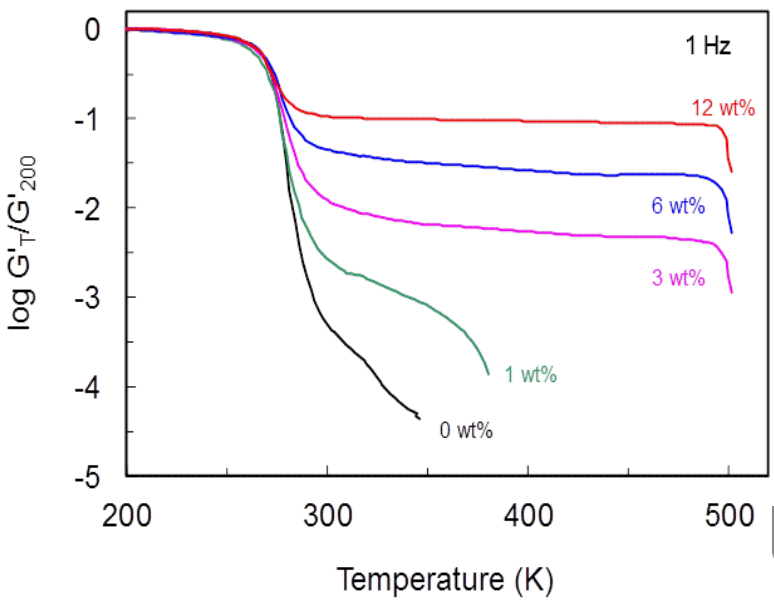


High reinforcing effect at T > Tg

Thermal stabilization up to 500 K ($\phi_R$ > 1wt%)
(degradation of cellulose)

Favier et al., *Polym. Adv. Technol.*, **1995**, 6, 351-355

# Morphology

Mean Field Approach: Halpin-Kardos

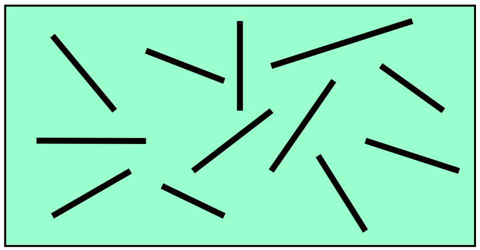

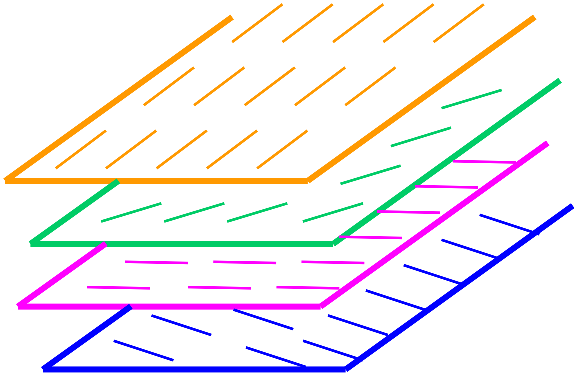

$$E_c = f(E_{ii}, G_{12}, \nu_{12}, \nu_{21})$$

$$\frac{E_{ii}}{E_m} = \frac{(1+\xi_{iif}\phi_f)E_{iif} + \xi_{ii}(1-\phi_f)E_m}{(1-\phi_f)E_{iif} + (\xi_{ii}+\phi_f)E_m} \quad (i=1,2)$$

$$\frac{G_{12}}{G_m} = \frac{(1+\phi_f)G_f + (1-\phi_f)G_m}{(1-\phi_f)G_f + (1+\phi_f)G_m}$$

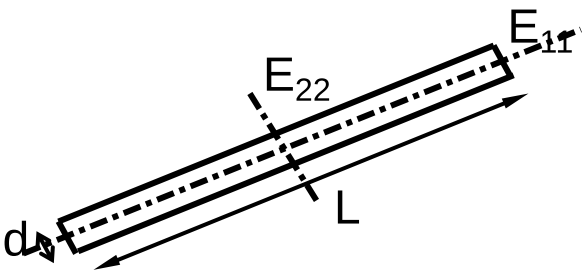


filler geometry : $\xi_{11} = 2 \times \frac{L}{d}$ $\quad \xi_{22} = 2 \times \frac{e}{d} = 2$

filler volume fraction : $\phi_f$

mechanical anisotropy : $E_{iif}$

no interaction between fibers

# Morphology

Mean Field Approach: Halpin-Kardos

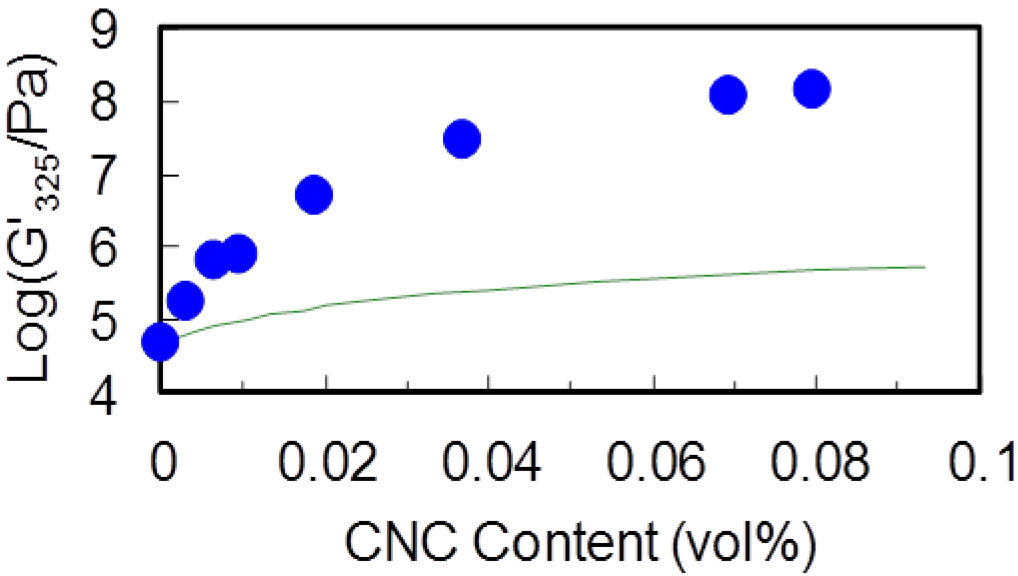


$L/d$ = 67 (TEM)

$\nu_m$ = 0.5 (rubbery matrix)

$G_m$ = 0.1 (experimental data)

$\nu_f$ = 0.3 (crystalline cellulose)

$E_{11f}$ = 150 GPa (theoretical data)

$E_{22f}$ = 15 GPa (theoretical data)

$G_f$ = 5 GPa (theoretical data)

Experimental data much higher than the prediction by a mean-field mechanical model

CNCs act as fibers much longer than expected from geometrical observation

# Morphology

Percolation Approach: Takayanagi Model

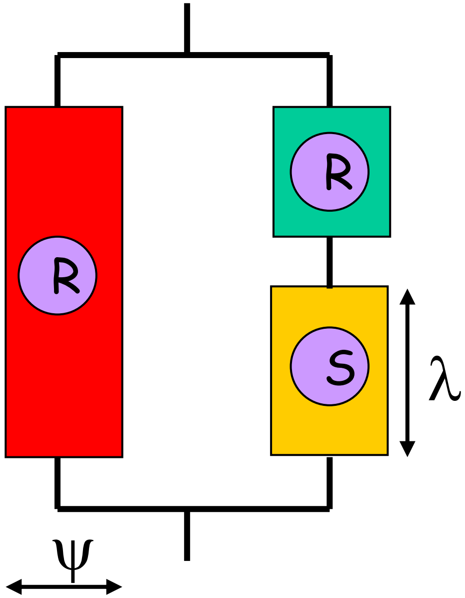


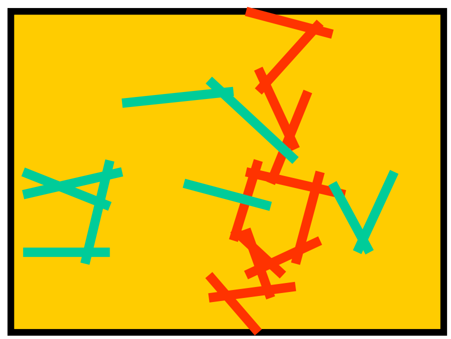

$$G = \frac{(1-2\psi+\psi\phi_R)G_S G_R + (1-\phi_R)\psi G_R^2}{(1-\phi_R)G_R + (v_R-\psi)G_S}$$

if $G_R >> G_S \Rightarrow G = \psi G_R$

$\psi = 0$ for $\phi_R < \phi_{Rc}$

$\psi = \phi_R \left(\frac{\phi_R - \phi_{Rc}}{1-\phi_{Rc}}\right)^b$ for $\phi_R \geq \phi_{Rc}$

percolating whiskers network :
$E_R$ = 15 GPa → $G_R$ = 5 GPa

L/d = 67 → $\phi_{Rc}$ = 1%
b = 0.4 (3D system)

$\psi$ = volume fraction of the percolating rigid phase
$\phi_R$ = volume fraction of filler
$\phi_{Rc}$ = critical volume fraction at the percolation threshold
b = critical exponent
$G_R$ = modulus of the percolating CNC network

Favier et al., *Polym. Adv. Technol.*, **1995**, 6, 351-355

# Morphology

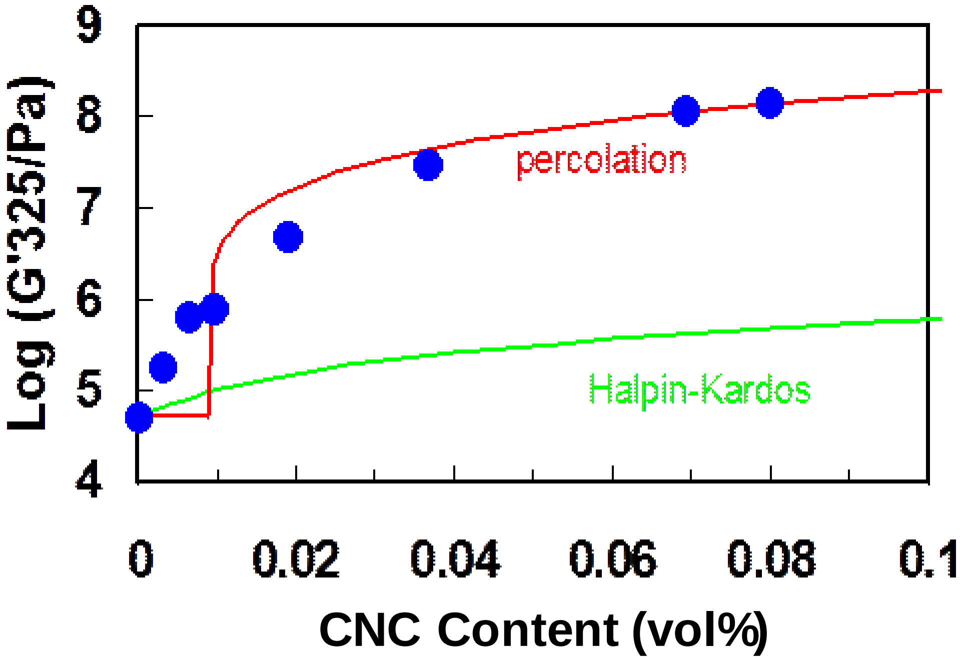


Favier et al., *Polym. Adv. Technol.*, **1995**, 6, 351-355

Good agreement between experimental and predicted data

Strong interactions between CNCs (H-bonding forces) → formation of a rigid cellulose CNC network for $\phi_R > \phi_{RC}$

**Mechanical percolation effect**

- High reinforcing effect
- Thermal stabilization of the composite modulus

(water evaporation = slow process)

LGP2

# Interphase

Tunicin CNC/amorphous PHO latex

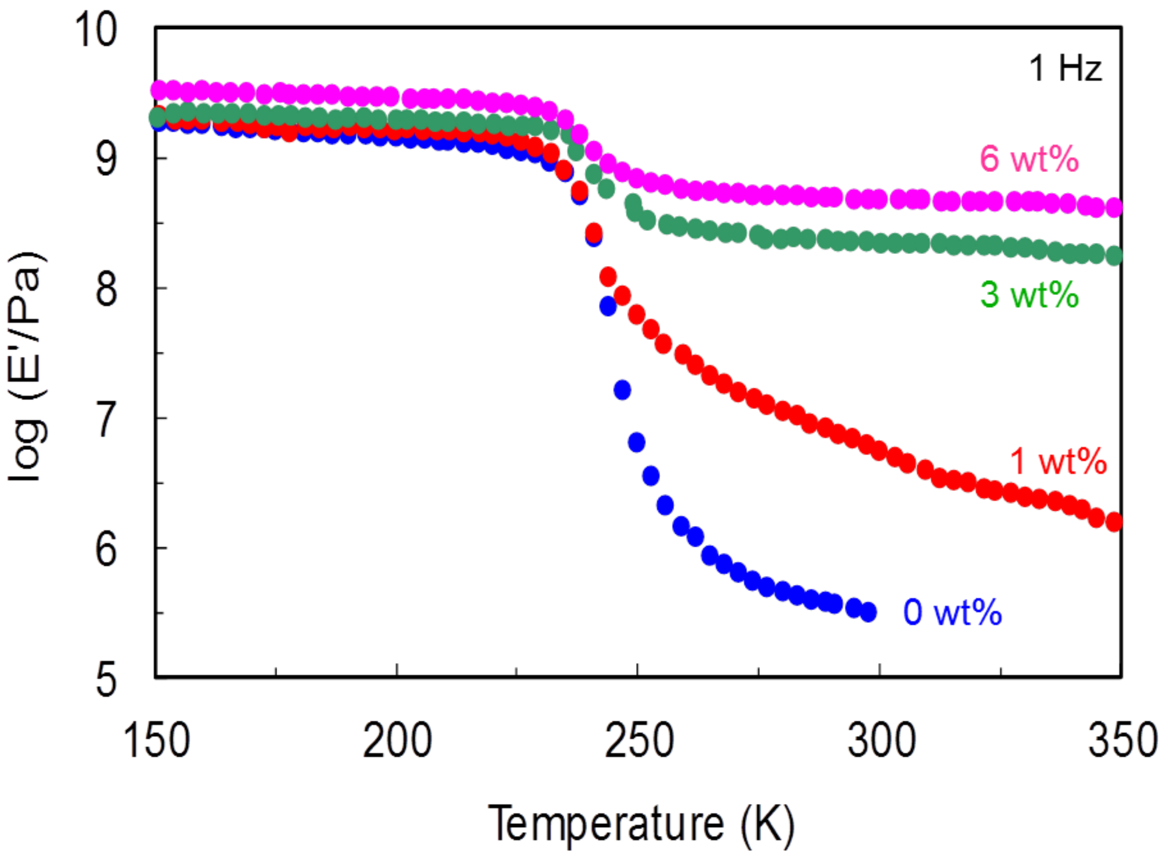


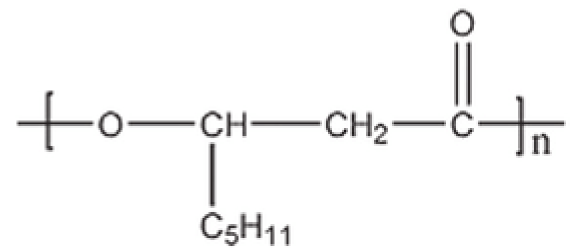


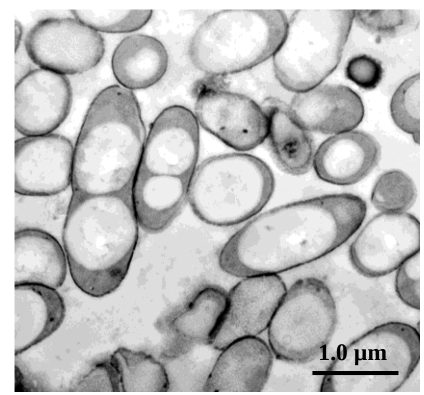


Dufresne and Samain, *Macromolecules* **1998**, 31, 6426-6433

Percolation

Dufresne, *Compos. Interfaces* **2000**, 7, 53-67

# Interphase

Tunicin CNC/semicrystalline PHO latex

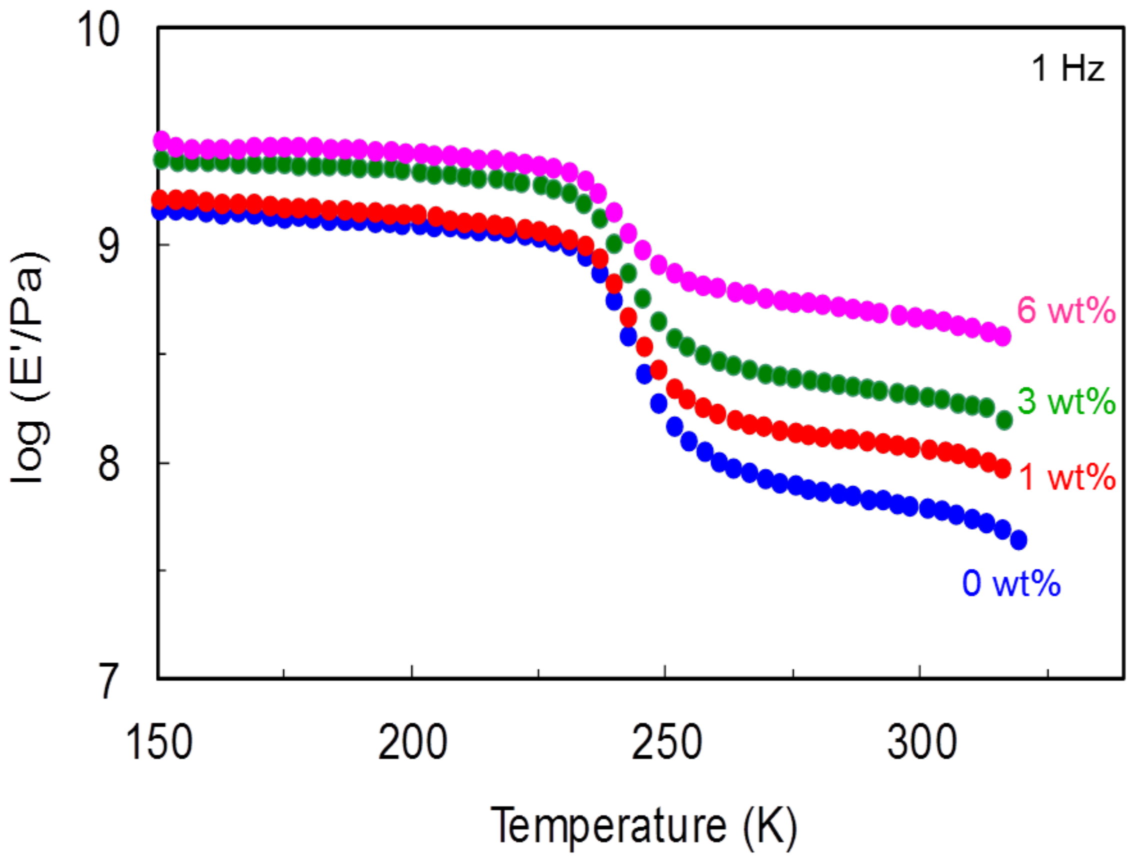


Global behavior similar except lower relative modulus increase

Crystalline domains = filler + physical crosslinks

Modulus decreases irremediably ~ 320 K (melting) regardless filler content

Dufresne, *Compos. Interfaces* **2000**, 7, 53-67

# Interphase

Tunicin CNC/amorphous PHO latex

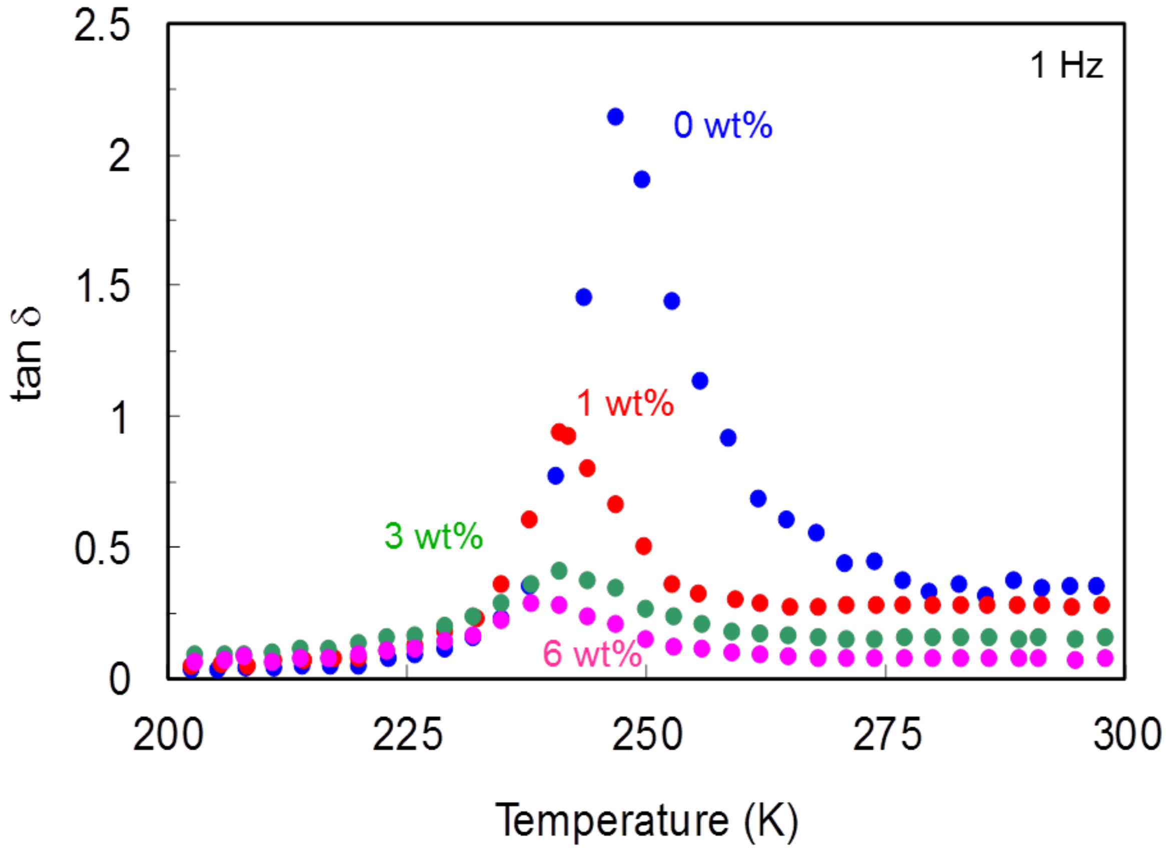


Magnitude of relaxation process decreases with CNC content

(i) number of mobile units

(ii) magnitude of modulus drop

(iii) interfacial effect

Dufresne, *Compos. Interfaces* **2000**, 7, 53-67

# Interphase

Tunicin CNC/semicrystalline PHO latex

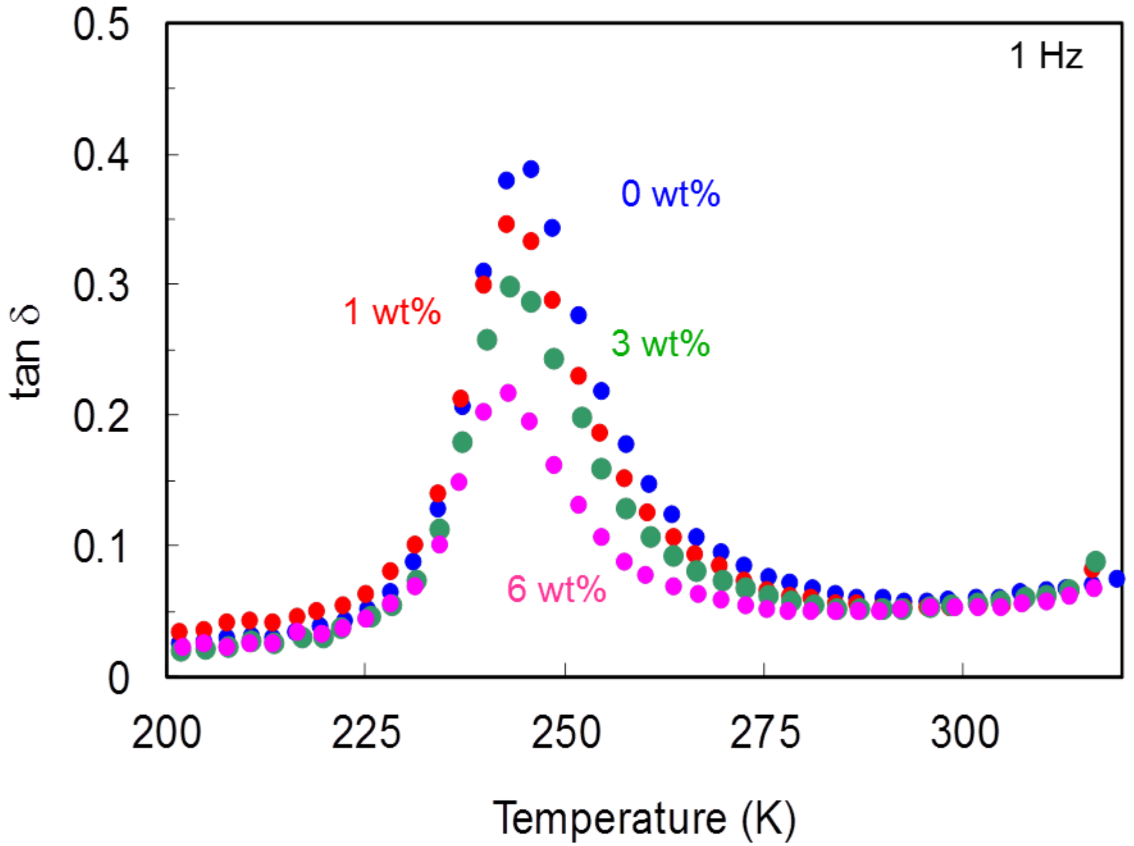


Similar observations

Dufresne, *Compos. Interfaces* **2000**, 7, 53-67

# Interphase – Loss Angle

Main characteristics deduced from the relaxation process displayed through the maximum of the loss angle

**Temperature position** = linked to Tg and to the magnitude of the modulus drop (mechanical coupling effect)

**Width** = representative of the size distribution of mobile entities participating to the relaxation process and distribution of relaxation times

**Magnitude** = related to the magnitude of the modulus drop and depends upon both the number of mobile entities and their contribution to the compliance

# Interphase – Loss Angle

| Matrix | CNC Content (wt%) | Tα (K) | Lα (K) | Iα |
|---|---|---|---|---|
| Amorphous PHO | 0 | 247 | 14 | 2.14 |
| | 1 | 241 | 16 | 0.938 |
| | 3 | 241 | 25 | 0.404 |
| | 6 | 240 | 21 | 0.290 |
| Semicrystalline PHO | 0 | 246 | 20 | 0.388 |
| | 1 | 243 | 19 | 0.346 |
| | 3 | 243 | 19 | 0.300 |
| | 6 | 243 | 20 | 0.216 |

Temperature position (Tα)
Half-height width (Lα)
Magnitude (Iα) of the α relaxation process

Dufresne, *Compos. Interfaces* **2000**, 7, 53-67

# Interphase – Loss Angle

| Matrix | CNC (wt%) | Tα (K) | Lα (K) | Iα |
|---|---|---|---|---|
| Am. PHO | 0 | 247 | 14 | 2.14 |
| | 1 | 241 | 16 | 0.938 |
| | 3 | 241 | 25 | 0.404 |
| | 6 | 240 | 21 | 0.290 |
| SC PHO | 0 | 246 | 20 | 0.388 |
| | 1 | 243 | 19 | 0.346 |
| | 3 | 243 | 19 | 0.300 |
| | 6 | 243 | 20 | 0.216 |

Shift of Tα towards lower temperatures with increasing CNC content

mechanical coupling effect

Temperature position (Tα)
Half-height width (Lα)
Magnitude (Iα) of the α relaxation process

# Interphase – Loss Angle

| Matrix | CNC (wt%) | Tα (K) | Lα (K) | Iα |
|---|---|---|---|---|
| Am. PHO | 0 | 247 | 14 | 2.14 |
| | 1 | 241 | 16 | 0.938 |
| | 3 | 241 | 25 | 0.404 |
| | 6 | 240 | 21 | 0.290 |
| SC PHO | 0 | 246 | 20 | 0.388 |
| | 1 | 243 | 19 | 0.346 |
| | 3 | 243 | 19 | 0.300 |
| | 6 | 243 | 20 | 0.216 |

Increase of Lα with crystallinity

coexistence of crystalline and amorphous chains (broader distribution of τ)

Temperature position (Tα)
Half-height width (Lα)
Magnitude (Iα) of the α relaxation process

# Interphase – Loss Angle

| Matrix | CNC (wt%) | Tα (K) | Lα (K) | Iα |
|---|---|---|---|---|
| Am. PHO | 0 | 247 | 14 | 2.14 |
| | 1 | 241 | 16 | 0.938 |
| | 3 | 241 | 25 | 0.404 |
| | 6 | 240 | 21 | 0.290 |
| SC PHO | 0 | 246 | 20 | 0.388 |
| | 1 | 243 | 19 | 0.346 |
| | 3 | 243 | 19 | 0.300 |
| | 6 | 243 | 20 | 0.216 |

Increase of Lα with CNC content for amorphous PHO

modification of mobility of amorphous PHO

Temperature position (Tα)
Half-height width (Lα)
Magnitude (Iα) of the α relaxation process

# Interphase – Loss Angle

| Matrix | CNC (wt%) | Tα (K) | Lα (K) | Iα |
|---|---|---|---|---|
| Am. PHO | 0 | 247 | 14 | 2.14 |
| | 1 | 241 | 16 | 0.938 |
| | 3 | 241 | 25 | 0.404 |
| | 6 | 240 | 21 | 0.290 |
| SC PHO | 0 | 246 | 20 | 0.388 |
| | 1 | 243 | 19 | 0.346 |
| | 3 | 243 | 19 | 0.300 |
| | 6 | 243 | 20 | 0.216 |

Decrease of Iα with CNC content

- decreasing number of mobile units
- possible chain adsorption
- dependence on the modulus drop

Temperature position (Tα)
Half-height width (Lα)
Magnitude (Iα) of the α relaxation process

# Interphase – Loss Angle

Specific surface of tunicin CNC ~ 170 $m^2.g^{-1}$

→ Interfacial effects are expected to be important

Yim *et al.*, 1973

$$\frac{I_{\alpha C}}{I_{\alpha M}} = 1 - v_R\left(1+\frac{\Delta R}{R_o}\right)^2\left(1+\frac{2\Delta R}{L}\right)$$

adsorption : effective filler volume fraction

+

Dufresne, 2000

$$\frac{I_{\alpha C}(cal)}{I_{\alpha C}(exp)} = \left(1+\frac{\Delta R}{R_o}\right)^2\left(1+\frac{2\Delta R}{L}\right)$$

mechanical coupling effect

$I_{\alpha C}$ = magnitude of loss angle for composite
$I_{\alpha M}$ = magnitude of loss angle for matrix
$v_R$ = volume fraction of filler

$R_o$, L = radius, length of fiber
$\Delta R$ = thickness of interphase

LGP2

# Interphase – Loss Angle

Modeling the viscoelastic behavior with the percolation approach

$$E_C{}^* = \frac{aE_S{}^* E_R + bE_R{}^2}{cE_S{}^* + dE_R} = E'_C + iE''_C$$

$a = 1-2\psi+\psi v_R$
$b = (1-v_R)\psi$
$c = v_R-\psi$
$d = 1-v_R$

$$E'_C = \frac{AC + BD}{C^2 + D^2} E_R \qquad E''_C = \frac{BC - AD}{C^2 + D^2} E_R$$

$A = aE_S' + bE_R$
$B = aE_S''$
$C = cE_S' + dE_R$
$D = cE_S''$

# Interphase – Loss Angle

Semicrystalline PHO

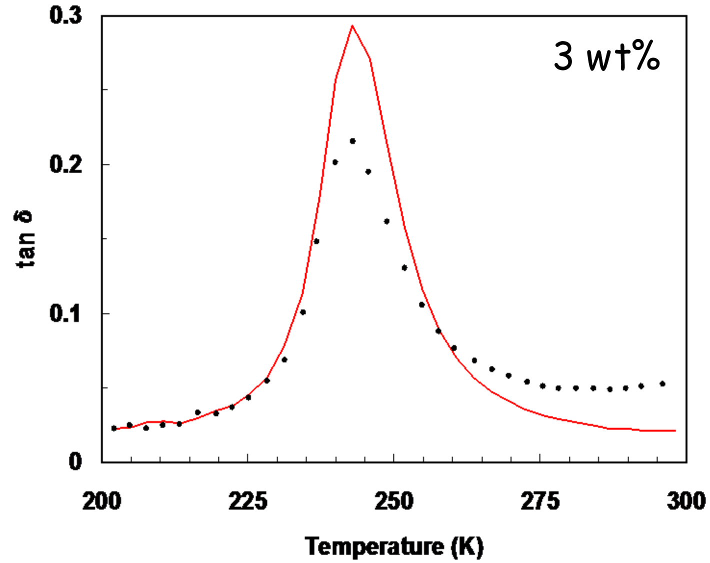


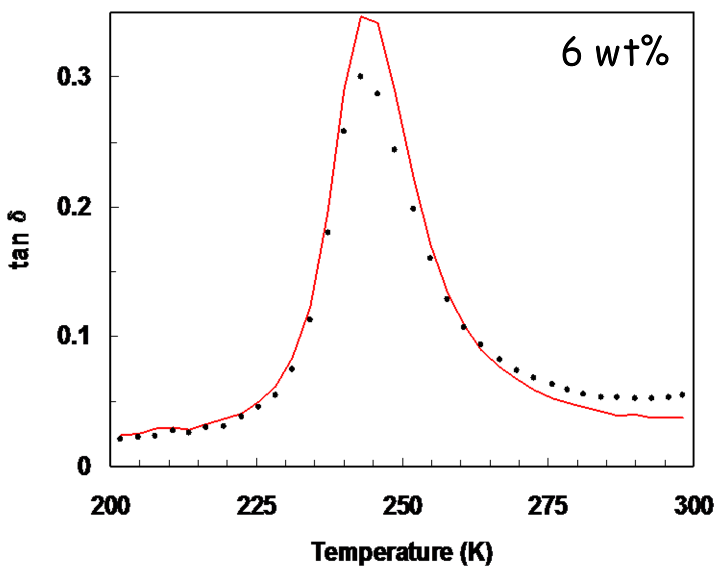


Rather good agreement between experimental and predicted values

→ the mobility of amorphous chains at the filler-matrix interface is not significantly affected

→ no direct contact between amorphous chains and CNCs

# Interphase – Loss Angle

Amorphous PHO

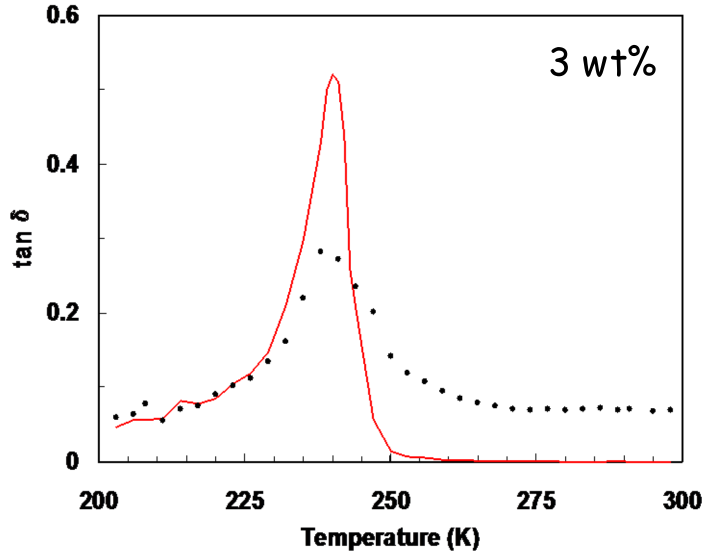


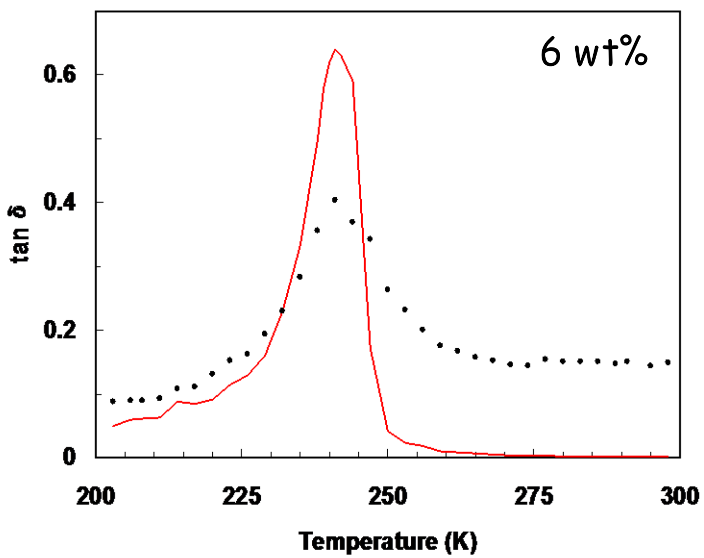


The model fails to describe the experimental data

→ the mobility of amorphous chains at the filler-matrix interface is affected

# Interphase – Loss Angle

| Matrix | CNC (wt%) | Tα (K) | Lα (K) | Iα | ΔR (nm) |
|---|---|---|---|---|---|
| Am. PHO | 0 | 247 | 14 | 2.14 | ___ |
| | 1 | 241 | 16 | 0.938 | ___ |
| | 3 | 241[241] | 25 [10] | 0.404 [0.640] | 3.8 |
| | 6 | 240 [240] | 21 [9] | 0.290 [0.52] | 5.0 |
| SC PHO | 0 | 246 | 20 | 0.388 | ___ |
| | 1 | 243 | 19 | 0.346 | ___ |
| | 3 | 243 [243] | 19 [18] | 0.300 [0.347] | 1.1 |
| | 6 | 243 [243] | 20 [16] | 0.216 [0.293] | 2.4 |

Temperature position (Tα)
Half-height width (Lα)
Magnitude (Iα) of the α relaxation process

[calculated data]

Agreement between exp. and predicted data much better for semicrystalline PHO based systems

Dufresne, *Compos. Interfaces* **2000**, 7, 53-67

# Interphase – Loss Angle

| Matrix | CNC (wt%) | Tα (K) | Lα (K) | Iα | ΔR (nm) |
|---|---|---|---|---|---|
| Am. PHO | 0 | 247 | 14 | 2.14 | ___ |
| | 1 | 241 | 16 | 0.938 | ___ |
| | 3 | 241[241] | 25 [10] | 0.404 [0.640] | 3.8 |
| | 6 | 240 [240] | 21 [9] | 0.290 [0.52] | 5.0 |
| SC PHO | 0 | 246 | 20 | 0.388 | ___ |
| | 1 | 243 | 19 | 0.346 | ___ |
| | 3 | 243 [243] | 19 [18] | 0.300 [0.347] | 1.1 |
| | 6 | 243 [243] | 20 [16] | 0.216 [0.293] | 2.4 |

Temperature position (Tα)
Half-height width (Lα)
Magnitude (Iα) of the α relaxation process

Dufresne, *Compos. Interfaces* **2000**, 7, 53-67

Ratio between exp. and predicted data

↓

Thickness of interphase

Interphase much thicker for amorphous matrix

↓

Presence of transcrystalline layer around CNC preventing any direct contact between amorphous PHO chains and CNC

# Cellulose Nanomaterials - CNC vs. CNF

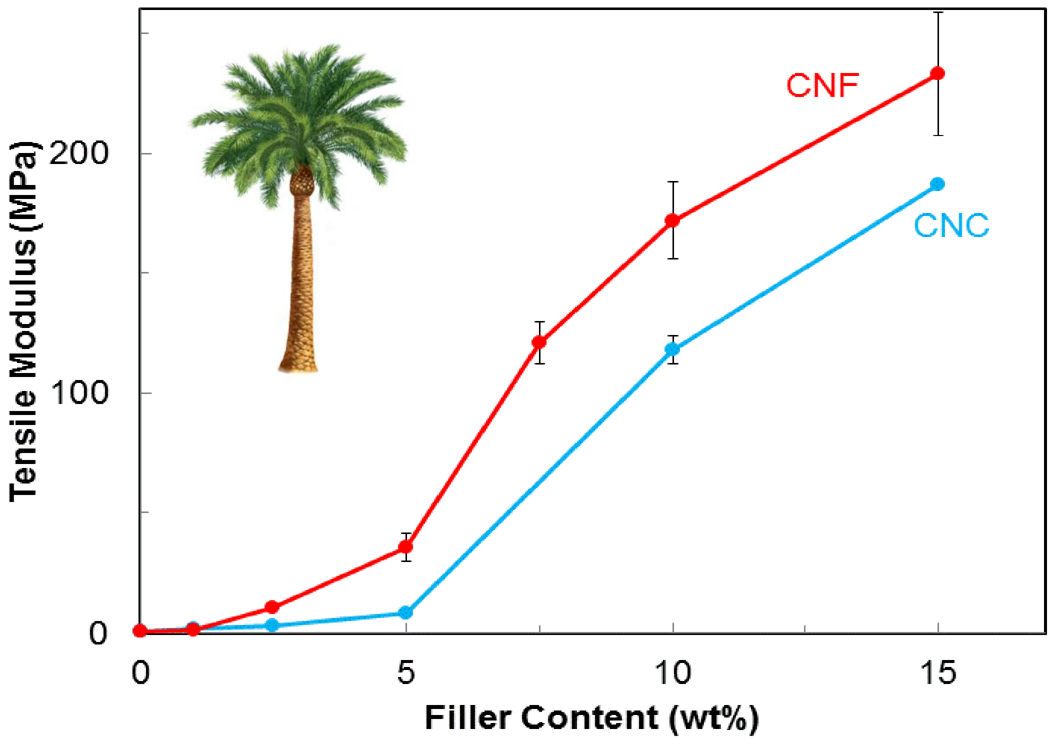


Palm tree CNC-CNF/NR

Higher modulus for CNF-based nanocomposites than for CNC-based nanocomposites

But higher modulus for CNC (130 GPa) than for CNF (100 GPa) ?

Bendahou et al., *Eur. Polym. J.* **2010**, 46, 609-620

# Cellulose Nanomaterials - CNC vs. CNF

- Higher aspect ratio for CNF → Connection of the nanoparticles for lower contents
- Entanglements → Stronger connection
- Residual hydrophobic compounds (lignin, extractive substances and fatty acids) at the surface of CNF → Compatibilization

Bendahou et al., *Eur. Polym. J.* **2010**, 46, 609-620

# Cellulose Nanomaterials - CNC vs. CNF

Residual hydrophobic compounds at the surface of CNF

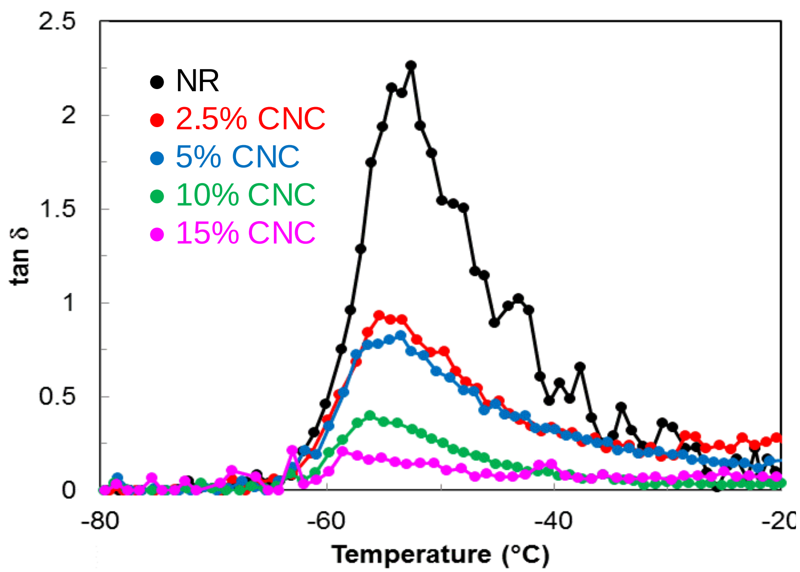


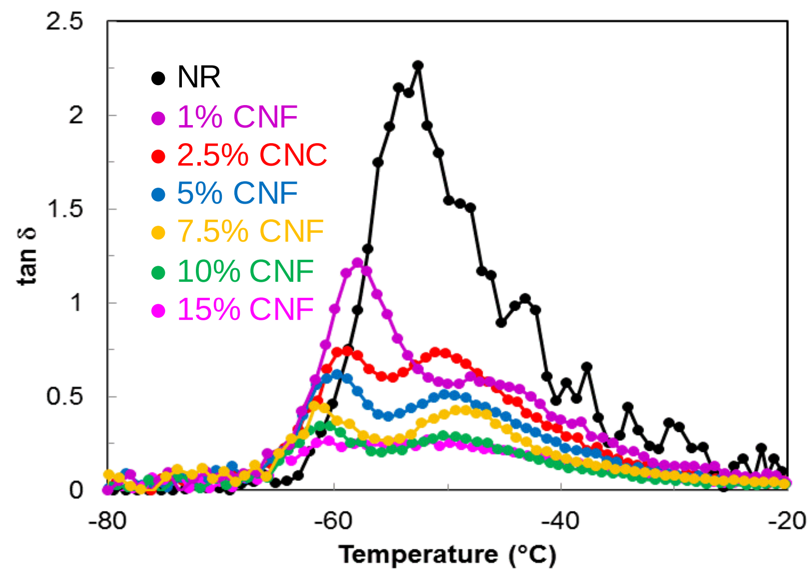


Splitting of the relaxation process ascribed to strong interactions between CNF and NR : formation of an interfacial layer with restricted mobility

Bendahou et al., *Eur. Polym. J.* **2010**, 46, 609-620

# Conclusion

Cellulose nanomaterials strongly impact the rheological behavior of suspensions/solid nanocomposites

Gel stiffness can be accessed

Solid state rheological characterization often used only to determine the glass-rubber transition temperature

Additional information can be obtained to characterize the microstructure/ morphology and interfacial effects

# Thank you for your attention

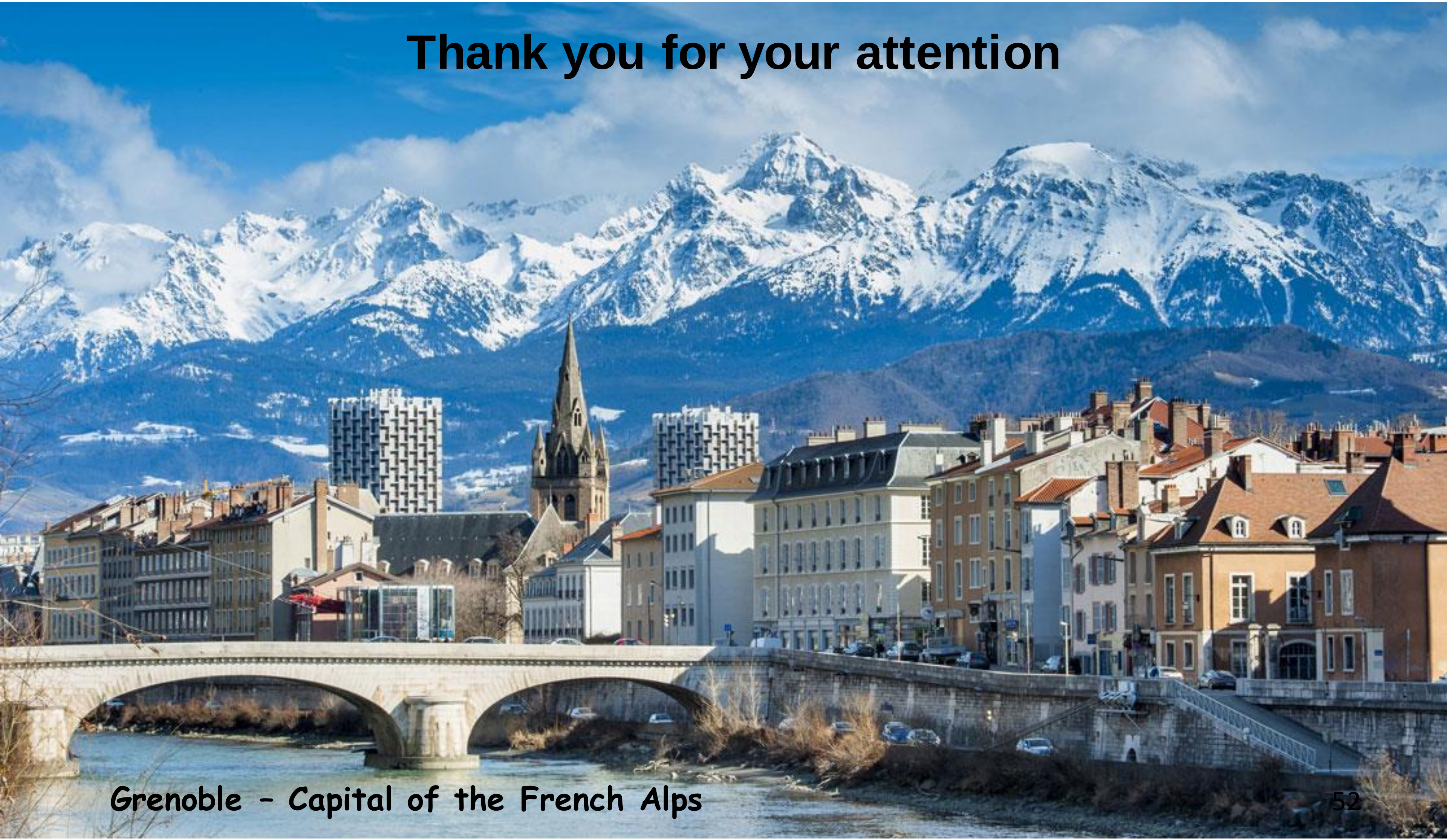

Grenoble – Capital of the French Alps